



¹⁰
I29 G
#31
e.1
CIVIL ENGINEERING STUDIES

HYDRAULIC ENGINEERING RESEARCH SERIES NO. 31

THEORETICAL FLUID FORCES ON IDEALIZED OCEAN STRUCTURES

RECEIVED

MAY 24 1978

C. E. REFERENCE ROOM

Metz Reference Room
Civil Engineering Department
B106 C. E. Building
University of Illinois
Urbana, Illinois 61801

By
J. P. MURTHA

A Technical Report of
Research Sponsored by the
NATIONAL SCIENCE FOUNDATION
Under Grant No. ENG 73-03677A01

DEPARTMENT OF CIVIL ENGINEERING
UNIVERSITY OF ILLINOIS AT URBANA-CHAMPAIGN
URBANA, ILLINOIS
JANUARY 1978

BIBLIOGRAPHIC DATA SHEET		1. Report No. UILLU-ENG-78-2007	2.	3. Recipient's Accession No.
4. Title and Subtitle Theoretical Fluid Forces on Idealized Ocean Structures				5. Report Date December 1977
				6.
7. Author(s) J. P. Murtha				8. Performing Organization Repr. No. HRS
9. Performing Organization Name and Address University of Illinois at Urbana-Champaign Urbana, Illinois 61801				10. Project/Task/Work Unit No.
				11. Contract/Grant No.
12. Sponsoring Organization Name and Address National Science Foundation Washington, D.C. 20550				13. Type of Report & Period Covered
				14.
15. Supplementary Notes				
16. Abstracts The report discusses theoretical elements of fluid-structure interaction forces on simple elements which are representative of members used in offshore structure. The elements used are vertical cylinders. The forces computed are based on ideal fluid theory. The loading condition treated are those associated with periodic surface waves and earthquakes.				
17. Key Words and Document Analysis. 17a. Descriptors Wave forces, Earthquakes forces, Ocean Structures, Ideal fluid theory				
17b. Identifiers/Open-Ended Terms Metz Reference Room Civil Engineering Department B106 C. E. Building University of Illinois Urbana, Illinois 61801				
17c. COSATI Field/Group				
18. Availability Statement Release unlimited		19. Security Class (This Report) UNCLASSIFIED		21. No. of Pages
		20. Security Class (This Page) UNCLASSIFIED		22. Price

ACKNOWLEDGEMENT

This report was prepared with the assistance of Messers. C. Ingram, A. Haas, and P. Fennel, Research Assistants in the Department of Civil Engineering at the University of Illinois at Urbana-Champaign. Mrs. M. Johnson and Miss H. Dillman typed the manuscript. Their assistance is greatly appreciated.

The investigation was sponsored by the National Science Foundation under grant number

The numerical results were obtained with the use of the IBM 360/75 computer system of the Computing Services Office of the University of Illinois at Urbana-Champaign.

TABLE OF CONTENTS

Chapter		Page
1	INTRODUCTION	1
	1.1 Introduction	1
	1.2 Description of Basic Problems	3
	1.3 Summary of Previous Studies	6
	1.4 Scope of the Present Study	8
	1.5 Nomenclature	8
2	THEORETICAL SOLUTION	13
	2.1 Introduction	13
	2.2 Incident Wave Description	15
	2.3 Equation of Motion of Test Rod	16
	2.4 General Solution for the Velocity Potential	18
	2.5 Evaluation of Coefficients $B_{m,n}$ and C_n	23
	2.6 Summary of the Solution	26
3	FORCES ACTING ON A STATIC STRUCTURE	30
	3.1 Introduction	30
	3.2 Static Forces	30
4	FORCES ASSOCIATED WITH DYNAMIC STRUCTURAL RESPONSE	34
	4.1 Introduction	34
	4.2 Single Degree of Freedom System	34
	4.3 Radiation Damping Force	36
	4.4 Added Mass Force	38
	4.5 Fluid-Structure Interaction Forces for the Translational Mode	40
5	RESPONSE OF OFFSHORE STRUCTURES TO EARTHQUAKES	42
	5.1 Introduction	42
	5.2 Modal Equations of Motion	42
	5.3 Approximate Expressions for Radiation Damping	48
6	SUMMARY	51
	BIBLIOGRAPHY	79

LIST OF FIGURES

<u>Figure</u>	<u>Title</u>	<u>Page</u>
1.1	Sketch of Single Degree-of-Freedom System for Free Surface Fluid-Structure Interaction Problems.	53
1.2	Coordinate Systems.	54
3.1	Relationship Between the Inertia Force Coefficient, C_I , and the Ratio of Cylinder Diameter to Incident Wave Length, D/λ .	55
3.2	Relationship Between the Inertia Force Coefficient, C_I , and Relative Depth Parameter, d/gT^2 ; for Various Values of the Ratio of Cylinder Diameter to Water Depth, D/d .	56
3.3	Relationship Between the Phase Lag, ν , of the Inertia Force with Respect to the Fluid Particle Acceleration and the Ratio of Cylinder Diameter to Incident Wave Length, D/λ .	57
3.4	Relationship Between the Phase Lag, ν , of the Inertia Force with Respect to the Fluid Particle Acceleration and Relative Depth Parameter, d/gT^2 , for Various Values of the Ratio of Cylinder Diameter to Incident Wave Length, D/d .	58
4.1	Relationship Between the Radiation Damping Coefficient, C_r , and the Relative Depth Parameter, d/gT^2 , for Various Ratios of Cylinder Diameter to Water Depth, D/d Triangular Mode Shape.	59
4.2	Relationship Between the Ratio of Radiation Damping Force Moment Arm to Water Depth, \bar{z}_r/d , and the Relative Depth Parameter, d/gT^2 .	60
4.3	Relationship Between the Coefficient c'_r and the Relative Depth Parameter, d/gT^2 . $c'_r = 2/\{\pi(kR)^2 \{(J'_1[kR])^2 + (Y'_1[kR])^2\}\}$	61
4.4	Relationship Between the Coefficient c''_r and the Relative Depth Parameter, d/gT^2 . $c''_r = (I_3/I_4) (\sinh[kd]/kd)$	62
4.5	Relationship Between the Added Mass Coefficient, C_M , and the Relative Depth Parameter, d/gT^2 , for Various Ratios of Cylinder Radius to Water Depth, D/d Triangular Mode Shape.	63

<u>Figure</u>	<u>Title</u>	<u>Page</u>
4.6	Relationship Between the Ratio of Added Mass Force Moment Arm to Water Depth, \bar{z}/d , and the Relative Depth Parameter, d/gT^2 , for Various Ratios of Cylinder Diameter to Water Depth, D/d . Triangular Mode Shape.	64
4.7	Relationship Between Added Mass Intensity Coefficient, c_m , and Dimensionless Depth, z/d for a Cylinder Diameter to Water Depth Ratio, D/d of 0.10 and Various Values of the Relative Depth Parameter, d/gT^2 . Triangular Mode Shape.	65
4.8	Relationship Between Added Mass Intensity Coefficient, c_m , and Dimensionless Depth, z/d , for a Cylinder Diameter to Water Depth Ratio, D/d , of 0.6 and Various Values of the Relative Depth Parameter, d/gT^2 . Triangular Mode Shape.	66
4.9	Relationship Between the Added Mass Intensity Coefficient, c_m , and Dimensionless Depth, z/d , for a Cylinder Diameter to Water Depth Ratio, D/d , of 1.0 and Various Values of the Relative Depth Parameter, d/gT^2 . Triangular Mode Shape.	67
4.10	Relationship Between the Added Mass Intensity Coefficient, c_m , and Dimensionless Depth, z/d , for a Relative Depth Parameter, d/gT^2 , of 0.001 and Various Values of the Ratio of Cylinder Diameter to Water Depth, D/d .	68
4.11	Relationship Between the Added Mass Intensity Coefficient, c_m , and Dimensionless Depth, z/d , for a Relative Depth Parameter, d/gT^2 , of Infinity and Various Values of the Ratio of Cylinder Diameter to Water Depth, D/d .	69
4.12	Relationship Between the Radiation Damping Coefficient, c_r , and the Relative Depth Parameter, d/gT^2 , for Various Ratios of Cylinder Diameter to Water Depth, D/d . Translational Mode Shape.	70
4.13	Relationship Between the Added Mass Coefficient, C_m , and the Relative Depth Parameter, d/gT^2 , for Various Ratios of Cylinder Radius to Water Depth, D/d . Translational Mode Shape.	71
4.14	Relationship Between the Ratio of Added Mass Force Moment Arm to Water Depth, \bar{z}/d , and the Relative Depth Parameter, d/gT^2 , for Various Ratios of Cylinder Diameter to Water Depth, D/d . Translational Mode Shape.	72

<u>Figure</u>	<u>Title</u>	<u>Page</u>
4.15	Relationship Between Added Mass Intensity Coefficient, c_m , and Dimensionless Depth, z/d , for a Cylinder Diameter to Water Depth Ratio, D/d , of 0.10 and Various Values of the Relative Depth Parameter, d/gT^2 . Translational Mode Shape.	73
4.16	Relationship Between Added Mass Intensity Coefficient, c_m , and Dimensionless Depth, z/d , for a Cylinder Diameter to Water Depth Ratio, D/d , of 0.4 and Various Values of the Relative Depth Parameter, d/gT^2 , Translational Mode Shape.	74
4.17	Relationship Between the Added Mass Intensity Coefficient, c_m , and Dimensionless Depth, z/d , for a Cylinder Diameter to Water Depth Ratio, D/d , of 1.0 and Various Values of the Relative Depth Parameter, d/gT^2 . Translational Mode Shape.	75
4.18	Relationship Between the Added Mass Intensity Coefficient, c_m , and Dimensionless Depth, z/d , for a Relative Depth Parameter, d/gT^2 of Infinity and Various Values of the Ratio of Cylinder Diameter to Water Depth, D/d . Translational Mode Shape.	76
5.1	Definition Sketch for Structure Subjected to Horizontal Ground Motion.	77
5.2	Idealized Structural Response Spectrum.	78

CHAPTER I

INTRODUCTION

1.1 INTRODUCTION

This report discusses theoretical aspects of fluid-structure interaction forces on simple elements which are representative of members used in offshore structures. These forces are those which may be computed from ideal, i.e., inviscid fluid theory. Originally, the purpose of the analysis was to assist in the development of fundamental laboratory experiments as well as the interpretation of experimental results. The problem under consideration was the determination of the dynamic response of simple, structural systems to water wave excitation. The related problem of response to earthquake excitation was subsequently incorporated into the analysis. Some of the results are of more general interest than the original intent, for example those considering the radiation damping associated with the response of offshore structures to earthquakes. Furthermore, the general solutions are useful in other problems involving fluid-structure interaction. Accordingly, the results of the study are summarized in this report.

The structures which motivated the study are those used in the development of offshore oil and gas resources. There are a variety of structures used for this purpose including the template and gravity types, and a common element in these structures is one constructed as a cylindrical cylinder. Thus the study of simple cylindrical members considered here is of value to the design of these structures.

The nature of the response problem may be illustrated by considering the response of a single degree-of-freedom(SDF) system subjected to water waves. Consider the system shown in Fig. 1-1. A rigid, cylindrical rod of length L is attached to the base by a moment-resisting spring. The rod is immersed in water with a depth d . The longitudinal axis of the rod is in the vertical direction.

Under the action of water waves the system will respond dynamically because of the fluid-structure interaction forces. These forces consist of three components according to ideal fluid theory. One force component depends only on the characteristics of the water wave and the geometry of the solid member. The second and third components are functions of the angular velocity and acceleration of the rod respectively. These latter components also depend on the geometry of the solid member. Since the first component is independent of the rod motion, it may be viewed as the wave force which would act on a static structure, i.e., a structure at rest; the component dependent upon the acceleration of the rod is associated with the so called "added mass" concept; and that dependent upon the velocity of the rod is associated with the "radiation damping" concept. The essential information pertaining to fluid-structure interaction forces in this problem may be obtained by solving two separate problems, viz:

- (1) THE STATIC PROBLEM - The computation of the forces produced by an incident surface wave on a rigid structure wave which responds statically to the excitation.
- (2) THE DYNAMIC PROBLEM - The computation of the forces produced by motion of the structure through the water when no other excitation acts on it.

If one wished to have the complete "solution" for motion of the rod when excited by surface waves, it could be developed by a combination of the two problems noted above. However, the solution of these problems may be interpreted in the form of a fluid inertia force coefficient, added mass coefficient, and radiation damping coefficient. These coefficients are the primary results presented in this report.

Since the second problem noted above pertains to the motion of the structure when the liquid is otherwise at rest, it is apparent that information pertaining to fluid-structure interaction forces associated with horizontal earthquake motion may be determined with only slight changes in the analysis. Accordingly, structural response to both surface waves and horizontal earthquake motion is considered in this report. In the case of response to water waves, the appropriate motion of the structure to be used, of course, is that associated with immovable seabed. In the case of horizontal earthquake motion, the motion of the seabed is the primary excitation.

1.2 DESCRIPTION OF BASIC PROBLEMS

The three basic problems described above may be formulated in analytical terms for simple single degree-of-freedom systems in the following manner. Let the coordinate system be that given in Fig. 1.2 in which the origin of the cartesian coordinates (x,y,z) is located at the seabed. The mean water depth is d . The cylindrical coordinates (θ,r,z) are as shown in the figure. According to ideal fluid theory, the analytical problem at hand is to find the potential function, ϕ , such that Laplace's equation is satisfied, viz: in cartesian coordinates

$$\frac{\partial^2 \Phi}{\partial x^2} + \frac{\partial^2 \Phi}{\partial y^2} + \frac{\partial^2 \Phi}{\partial z^2} = 0 \quad (1.2-1)$$

or in cylindrical coordinates,

$$\frac{\partial^2 \Phi}{\partial r^2} + \frac{1}{r} \frac{\partial^2 \Phi}{\partial \theta^2} + \frac{\partial^2 \Phi}{\partial z^2} = 0 \quad (1.2-2)$$

which are of more interest in the present work. Then the fluid, particle velocities in the radial, tangential, and vertical directions are u_r , u_θ , u_z respectively; and they are computed as follows.

$$u_r = - \frac{\partial \Phi}{\partial r} \quad (1.2-3)$$

$$u_\theta = - \frac{1}{r} \frac{\partial \Phi}{\partial \theta} \quad (1.2-4)$$

$$u_z = - \frac{\partial \Phi}{\partial z} \quad (1.2-5)$$

At the seabed (i.e., $z=0$) the boundary condition to be satisfied is

$$u_z = 0 \quad (1.2-6)$$

and the boundary conditions at the free water surface (i.e., $z=d$) are

$$\frac{\partial^2 \Phi}{\partial t^2} + g \frac{\partial \Phi}{\partial z} = 0 \quad (1.2-7a)$$

$$\eta = \frac{1}{g} \frac{\partial \Phi}{\partial t} \quad (1.2-7b)$$

according to Lamb (1)¹ where t is time.

(1) Numbers in parenthesis refer to entries in the Bibliography.

The additional boundary conditions to be satisfied depend upon the specific problem at hand. Let the single degree-of-freedom system of interest be a right circular cylinder of radius R and with a longitudinal axis coincident with the z -axis.

In the Static Problem the additional boundary conditions are that $u_r = 0$ at $r = R$ and that the wave motion on the free surface approach that of the incident wave field at large distances from the cylinder.

The force coefficients associated with the Dynamic Problem can be developed by examining the results on an SDF system of an impressed harmonic motion of specified frequency. In this case the appropriate boundary conditions are the compatibility of velocity at the boundary of the water and solid structure, and the fact that the water motion produced by the motion of the solid must vanish for large values of the radial coordinate. In dealing with multi degree-of-freedom (MDF) systems, the force coefficients are dependent on the mode shape as well as the excitation frequency, water depth, structural geometry and gravity.

The boundary conditions used in the Earthquake Response Problem are similar to those noted for the Dynamic Problem.

In the study of surface wave phenomena it is convenient frequently to use the concept of relative water depth. The parametric representation of this concept may be the ratio of water depth to wave length, d/λ ; the product of the wave number and water depth, $kd = 2\pi d/\lambda$; or the ratio d/gT^2 where g is the gravitational acceleration and T is the wave period. The parameter most used in this report as the relative depth parameter is d/gT^2 . In terms of these parameters, "shallow" water may be interpreted as $d/\lambda \leq 1/20$, $kd \leq \pi/10$, or $d/gT^2 \leq 0.0025$. "Deep"

water refers to $d/\lambda \geq 1/2$, $kd \geq \pi$ or $d/gT^2 \geq 0.08$. Between these two extremes, the term "intermediate" water depth is used frequently.

1.3 SUMMARY OF PREVIOUS STUDIES

Previous studies of interest in the present analysis may be divided into studies related to wave forces on static systems and fluid-structure interaction forces associated with simple dynamic systems. In all cases the water is treated as an inviscid fluid.

With regard to the subject of wave forces on a static system, Havelock (2) studied the hydrodynamic forces acting on an obstacle held in position in a train of plane periodic waves advancing over the surface of the water. He assumed that the water is incompressible and that the flow is irrotational. His work includes the wave forces acting on a vertical, cylindrical cylinder. Since Havelock's primary interest was with wave forces on ships, his solutions are limited to "deep" water i.e., $d/gT^2 > \sim 0.08$.

McCamy and Fuchs (3) considered the wave force acting on piles. They extended Havelock's solution to include all water depths. Their results are in agreement with those given in Chapter 3 of this report. The results given in Chapter 3 are in a different form which may be more useful for engineering analysis.

Spring and Monkmeyer (4) considered a similar problem except that they considered the wave forces acting on a series of equally-spaced vertical cylinders rather than a single cylinder. Their study was motivated by the need to assess confinement effects in tests conducted in wave flumes.

With regard to the study of fluid-structure interaction forces acting on simple dynamic systems, the two-dimensional analysis in rectangular coordinates was developed by Biesel et al. (5) in conjunction with the design of laboratory wave-generating equipment. They are concerned with the waves generated by periodic motion of a wave paddle in a flume. Their approach also takes the water to be an incompressible, inviscid fluid. They show clearly the effect of mode shape and excitation frequency in the form of the parameter d/gT^2 on the "added mass" force and the velocity-dependent force.

Petrauskas (6) conducted theoretical and experimental studies to determine the added mass and radiation damping of rigid cylinders. His analytical studies are similar to those presented here. They are based on ideal fluid potential theory and linear boundary conditions at the free surface. The circular cylinder stands in water of finite depth and pierces the free water surface. Experimental studies were conducted by imparting translational motion to the cylinder in water initially at rest. The measured added mass agreed well with predictions from ideal fluid theory. The measured radiation damping forces were on the average about 20 percent less than those predicted by theory.

He also conducted experimental studies on the added mass and drag force interaction for cylinders completely submerged and in free vibration in the presence of a steady current. Cylinder motions were small with respect to their diameter. The measured added mass agreed well with potential theory results. Theoretical and experimental drag force interaction results were somewhat different.

Liaw and Chopra (7) considered the hydrodynamic pressures on cylindrical "towers" surrounded by water and given a harmonic base excitation. Their analysis is also directed toward earthquake effects. Their analysis differs from the preceding ones in that they assume the fluid to be compressible. However, compressibility effects appear inconsequential except for very extreme cases. An earlier investigation pertaining to earthquake effects on cylindrical piers is that of Jacobsen (8).

1.4 SCOPE OF THE PRESENT STUDY

Chapter 2 outlines the general solution of the fluid-structure interaction coefficients for simple single degree-of-freedom systems. It contains the details of the mathematical solution. Section 2.6 is a summary of the solutions and gives the complete potential functions for the problems of interest.

Chapter 3 discusses the hydrodynamic forces acting on a static cylinder using the potential functions given in Chapter 2.

Chapter 4 presents the added mass and radiation damping coefficients associated with the response of the SDF system.

In Chapter 5, the theoretical solution given in Chapter 2 is adapted for the case of response of the SDF systems to earthquake excitation.

1.5 NOMENCLATURE

The nomenclature used in the report is listed here and defined again where it first appears in the text.

A_i = incident wave amplitude in complex form

A = amplitude of angular motion of the cylinder

$B_{m,n}$ = coef. in Eq. 2.21

B_m = special form of $B_{m,n}$ and defined in Eq. 2.54

c = wave speed

C_I = inertia force coefficient

C_M = added mass coefficient

C_R = radiation damping coefficient

C_0, C_1, C_n = coefficients defined in Eq. 2.43 a, b, and c respectively

C'_0, C'_n, C''_1 = coefficients defined in Eqs. 2.51, 2.52, and 2.53 respectively

C'_r, C''_i = coefficients defined in Eqs. 4.10 and 4.11 respectively

$C_{R,t}$ = translational mode radiation damping in earthquake response

$C_{R,i}$ = i-th mode radiation damping in earthquake response

$C_{M,t}$ = translational mode added mass coefficient in earthquake response

$C_{M,i}$ = i-th mode added mass coefficient in earthquake response

D = cylinder diameter

F_d = total hydrodynamic force due to rod motions

H = incident wave height

$H_n^{(1)}$ = Hankel function of the first kind of order $n = J + iY$

$H_n^{(1)'} = dH_n^{(1)}/d(kr)$

I_1, I_2, I_3, I_4 = integral expressions defined in Eqs. 2.57 through 2.60

$I'_3, I'_{\zeta i}, I'_1, I'_{\zeta i}$ = integral expressions defined in Eq. 5.9

I_s = moment of inertia of rod in air about axis through the base

J_n = Bessel function of the first kind of order n

$J'_n = dJ_n/d(kr)$

K_m = modified Bessel function of the second kind of order m

$K'_m = dK_m/d(kr)$

L = length of the rod

M = moment of fluid forces about the base

M_d = total mass of water displaced

M_{ai}^* = i -th modal mass in air

M_{di} = defined in Eq. 5.11

$M_t^*, M_{\zeta i}^*$ = defined in Eq. 5.12 and 5.13

R = radius of the rod

T = wave period

T_s = structural period

V = earthquake spectrum Psuedo-Velocity

W = weight of the rod in air

Y_n = Bessel function of the second kind, order n

$Y'_n = dY_n/d(kr)$

a = wave amplitude

c_s = structural damping coefficient

c_r = radiation damping intensity coefficient

c_m = added mass intensity coefficient

d = mean water depth

f_s = structural frequency in hertz

f_o = force intensity on a cylinder at rest

f_t = total force intensity on a cylinder

f_d = force intensity resulting from motion of the cylinder

$i = \sqrt{-1}$

k = wave number

k_n = defined in Eq. 2.22

m_d = mass of water displaced per unit length of cylinder

p = total fluid pressure

p_h = hydrostatic pressure

- p_d = hydrodynamic pressure
 q, \dot{q}, \ddot{q} = generalized displacement, velocity, and acceleration
 r, θ, z = cylindrical coordinate
 t = time
 u = horizontal fluid particle velocity in rectangular coordinate
 u_r, u_θ, u_z = particle velocity components in cylindrical coordinates
 x, y, z = rectangular coordinates
 x, \dot{x}, \ddot{x} = relative displacement, velocity, and acceleration in earthquake response
 $x_o, \dot{x}_o, \ddot{x}_o$ = ground motion displacement, velocity, and acceleration in earthquake motion
 $x_s, \dot{x}_s, \ddot{x}_s$ = absolute structural displacement, velocity, and acceleration in earthquake motion
 z_c = c.g. of the rod above the base
 \bar{z}_m = centroid distance of the added mass
 Γ_{ai} = participation factor in air
 Γ_{wi} = participation factor in water
 Φ = potential function
 Φ_i = incident wave potential
 Φ'_o = radiated wave potential for static structural response
 Φ''_o = radiated wave potential for dynamic structural response
 Φ_s = standing wave potential
 λ = wave length
 $\alpha, \dot{\alpha}, \ddot{\alpha}$ = angular displacement, velocity, and acceleration of a rigid rod
 β_{ai} = structural damping ratio in air, i^{th} mode
 β_{wi} = structural damping ratio in water, i^{th} mode
 σ = mass density of water
 v = phase angle
 η = elevation of free water surface above the mean water level

σ = circular frequency

ω = undamped structural frequency

ω_d = damped structural frequency

ζ_{ai} = i^{th} mode shape in air

ζ_{wi} = i^{th} mode shape in water

CHAPTER 2

THEORETICAL SOLUTION

2.1 INTRODUCTION

The objective of this chapter is to outline the general solution for the fluid-structure interaction coefficients for simple single degree-of-freedom systems excited by water waves. Accordingly this chapter provides the basic equations for the problems discussed in Chapter I. These equations are summarized completely in Section 2.6. Other sections of this chapter are concerned with the details of the mathematical solution. The analysis presented herein is based on the assumption that the fluid is inviscid and incompressible and that its motion is irrotational. Linear wave theory is assumed to describe the incident and structure-generated water waves, and the motion of the solid body is assumed to be small with respect to the water depth.

The solid body is the simple single degree-of-freedom system shown in Fig. 1.1 which resembles closely the laboratory specimen used in the experimental program. It is a right circular cylindrical rod attached to the laboratory flume floor by a hinge and supported by an elastic spring above the free water surface. The rod is rigid and its longitudinal axis is in the vertical direction.

The objective of the analysis is to determine, according to the assumptions given, the force intensity or force per unit length acting on the vertical cylinder because of water motion and the induced motion of the rod.

The results of the analysis show that the interaction force may be viewed as consisting of three parts: viz, one part which is independent of the rod motion, a second part proportional to the angular velocity of the rod, and a third part proportional to the angular acceleration of the

rod. The first component of the interaction force, being independent of the rod motion, is the wave force which would act on a static structure.

If both the water and the rod were at rest and the rod then excited, the motion of the rod would alter the energy of the fluid. For example, if the top of the rod is moved in harmonic motion, a progressive wave is generated by its motion and is propagated outward from the cylinder. In addition, this excitation produces a standing wave also in the fluid near the cylinder. The interaction force associated with the production of these two waves has a component proportional to the angular acceleration of the rod and one proportional to angular velocity. The first of these components, because of the proportionality to acceleration, is commonly called the "added mass". The second component may be termed "radiation damping" since it will appear in the equation of motion of the rod as a dissipative term proportional to the first power of velocity. More precise definitions of these terms will be given later.

When the rod is set into motion by the action of waves rather than some external cause, the "added mass" and "radiation damping" effects are superposed on the interaction force component associated with wave forces on a static rod.

It may be useful to recall here that the present analysis assumes a non-viscous fluid, and hence, will not predict the existence of a drag type interaction force component proportional to the square of the relative velocity of a point on the rod measured with respect to the fluid.

In the following discussion the basic equations will be developed for computing interaction forces for the simple rod. In subsequent chapters the force intensity will be determined first for the rod and then the

expressions will be modified to put the results in more general form useful in predicting the response of actual structures.

2.2 INCIDENT WAVE DESCRIPTION

According to linear wave theory (9) a long-crested, progressive, periodic wave of amplitude a and circular σ , and propagating in water of constant depth d is defined by the following equations

$$\phi_i = \frac{ag}{\sigma} \frac{\cosh[kz]}{\cosh[kd]} \cos [kx - \sigma t] \quad (2.1)$$

$$\eta_i = a \sin [kx - \sigma t] \quad (2.2)$$

$$\sigma^2 = gk \tanh [kd] \quad (2.3)$$

The incident wave velocity potential is ϕ_i , a is the wave amplitude, g is the gravitational acceleration, σ is the circular wave frequency, k is the wave number, d is the water depth, and η is the elevation of the free water surface above the mean water level. The coordinate systems x, y, z and r, z, θ are shown in Fig. 1.2. Time is denoted t . The quantities σ , k , and a are related to the wave period T , wave length λ , and the wave height H respectively by the following relationship

$$\sigma = \frac{2\pi}{T} \quad (2.4)$$

$$k = \frac{2\pi}{\lambda} \quad (2.5)$$

$$a = \frac{H}{2} \quad (2.6)$$

The wave described here travels in a direction parallel to the x-axis with a wave speed or celerity C where

$$C = \frac{\sigma}{k} \quad (2.7)$$

It is more convenient to adopt cylindrical coordinates as well as complex algebra notation. Accordingly, the incident wave potential may be taken as the real part of the following expression.

$$\phi_i = A_i \cosh[kz] \{ J_0[kr] + 2 \sum_{n=1}^{\infty} i^n J_n[kr] \cos[n\theta] \} \exp[-i\sigma t] \quad (2.8)$$

and

$$A_i = \frac{ag}{\sigma \cosh[kd]} \quad (2.9)$$

The quantity J_n is the Bessel Function of the first kind of order n and i is equal to $\sqrt{-1}$.

2.3 EQUATION OF MOTION OF TEST ROD

The single degree-of-freedom system is shown in Fig. 1.1. It is a circular, rigid rod section. For the purpose of this analysis, the rod is assumed to move only in the x-z plane, and its displaced configuration is defined by the angle α measured clockwise from the vertical axis. Accordingly, the rod is a single-degree-of-freedom system and the equation of motion for small angles of displacement is as follows.

$$I_s \ddot{\alpha} + c_s \dot{\alpha} + (k_s L^2 - W z_c) \alpha = M \quad (2.10)$$

The mass moment of inertia of the rod in air about an axis through the bottom hinge is I_s , c_s is a coefficient of friction accounting for energy loss in the solid parts the assembly, the spring constant is k_s , the total weight of the rod in air is W and z_c is the location of the center of gravity of the rod above the hinge. The moment of the fluid forces about the hinge is M .

The moment M is computed from the total fluid pressure, p_t , acting on the surface of the cylinder. If ϕ_t is the total velocity potential describing the fluid-rod interaction, the total pressure is given by the following

$$p_t = \rho \frac{\partial \phi_t}{\partial t} + \rho g (d-z) \quad (2.11)$$

where ρ is the mass density of water. The force intensity at any section, f_t , of the rod is given as follows.

$$f_t = -2 \int_0^\pi p_t R \cos [\theta] d\theta \quad (2.12)$$

The quantity R is the radius of the rod.

Finally, the moment is

$$M = \int_0^{d+\eta} f_t z dz = 2 \int_0^{d+\eta} \int_0^\pi \rho z \frac{\partial \phi_t}{\partial t} R \cos [\theta] d\theta dz \quad (2.13)$$

The second term on the right hand side of Eq. 2.11 is, of course, the hydrostatic pressure, p_h . The interaction force intensity associated with it is $\pi R^2 \rho g \alpha$ for small but finite values of α . There remains to compute the hydrodynamic force intensity, f_d , associated with the

hydrodynamic pressure p_d , where

$$p_d = \rho \frac{\partial \phi_t}{\partial t} \quad (2.14-a)$$

and

$$f_d = -2\rho R \int_0^\pi \frac{\partial \phi_t}{\partial t} \cos [\theta] d\theta \quad (2.14-b)$$

2.4 GENERAL SOLUTION FOR THE VELOCITY POTENTIAL

This section describes the general solution for the total velocity potential from which the interaction pressure may be computed. Accordingly, we seek solutions to Laplace's equation, viz

$$\nabla^2 \Phi = 0 = \frac{\partial^2 \Phi}{\partial r^2} + \frac{\partial^2 \Phi}{\partial z^2} + \frac{1}{r^2} \frac{\partial^2 \Phi}{\partial \theta^2} \quad (2.15)$$

which satisfy the following boundary conditions:

- (a) at $z = 0$, $\frac{\partial \Phi}{\partial z} = 0$
- (b) at $z = d$, $\frac{\partial^2 \Phi}{\partial t^2} + g \frac{\partial^2 \Phi}{\partial z^2} = 0$
- (c) at $r = R$, $-\frac{\partial \Phi}{\partial r} = z \dot{\alpha} \cos [\theta]$
- (d) at $r \rightarrow \infty$, $\Phi \rightarrow \Phi_i$

The first condition requires that the vertical velocity of fluid particles on the seabed be zero. The second condition requires constant pressure on the free water surface as well as the compatibility of free surface with

its constituent particles. The third condition relates the linear velocity of sections of the rod to the particle velocity of the fluid adjacent to the rod. Finally, the last condition requires that the spatial extent of the influence of the rod on the flow be finite.

The general solution for the total velocity potential can be determined by superimposing the potentials for the different wave types which can exist in the fluid medium in such a manner that the boundary conditions are satisfied. Accordingly, we need to combine the potential functions for a standing wave, ϕ_s , and a wave radiated outward, ϕ_o , with the incident wave given above. The total potential is then given by the following expression:

$$\phi = \phi_i + \phi_o + \phi_s \quad (2.16)$$

Note that the incident wave potential and associated relationships given in Eq. 2.1-2.3 and Eq. 2.8 and 2.9 satisfy the boundary conditions except at the surface of the rod. The potential functions given below for the standing and radiated waves are in the same manner; viz, they satisfy all the boundary conditions except at the rod. The boundary conditions at the rod and conditions of orthogonality are used to determine the unknown coefficients for the standing and radiated waves.

A simple wave propagating outward from the origin is defined by the following relationships.

$$\phi_o = \left\{ \sum_{n=0}^{\infty} C_n H_n^{(1)}[kr] \cos[n\theta] \cosh[kz] \right\} \exp[-i\sigma t] \quad (2.17)$$

$$\sigma^2 = gk \tanh [kd] \quad (2.18)$$

$$\bar{\eta}_0 = \left\{ \sum_{n=0}^{\infty} C_n H_n^{(1)} [kr] \cosh [kd] \cos [n\theta] \right\} \exp[-i\sigma t] \quad (2.19)$$

where the complex potential for the radiated wave is Φ_0 , the values of C_n are unknown coefficients, $H_n^{(1)}[\cdot]$ is the Hankel function of the first kind evaluated for the argument notes in brackets. The quantity $\bar{\eta}_0$ is the water surface elevation associated with this wave component given in complex form. Note that the relationship between circular frequency and wave number given by Eq. 2.18 is identical with that given by Eq. 2.3.

The progressive wave nature of Φ_0 can be observed easily by examining the product of the space and time terms for large values of r , i.e.,

$$H_n^{(1)} [kr] \exp[-i\sigma t] \approx \sqrt{\frac{2}{\pi kr}} \exp[-i(kr - \sigma t - \frac{\pi}{4} - \frac{\eta\pi}{2})] \quad (2.20)$$

which is of the form $r - Ct$ and thus satisfies the requirement of a progressive wave.

As in the case of the incident wave, Eq. 2.17 satisfies all the boundary conditions except at the surface of the rod. This remaining boundary condition will be used later to compute the values of C_n .

The complex form of the velocity potential and associated equation for a standing wave, Φ_s , is as follows.

$$\Phi_s = \left\{ \sum_{m=0}^{\infty} \sum_{n=1}^{\infty} B_{m,n} K_m [k_n r] \cos [k_n z] \cos [m\theta] \right\} \exp[-i\sigma t] \quad (2.21)$$

$$\sigma^2 = -gk_n \tan [k_n d] \quad (2.22)$$

$$\bar{\eta}_s = \left\{ \sum_{m=0}^{\infty} \sum_{n=1}^{\infty} (-i\sigma) K_m[k_n r] \cos [k_n d] \cos [n\theta] \right\} \exp[-i\sigma t] \quad (2.23)$$

The quantity $B_{m,n}$ denotes a set of coefficients to be determined by the satisfaction of the remaining boundary condition, and $K_m[\cdot]$ is the modified Bessel function of the second kind of order m . Note that the free surface boundary condition results in a different relationship involving the circular frequency of the wave in Eq. 2.22 than that given for the incident or radiated waves in Eq. 2.3 or 2.18. Eq. 2.22 can be rewritten as follows.

$$\frac{\sigma^2 d}{g} = 4\pi^2 \frac{d}{gT^2} = -k_n d \tan [k_n d] \quad (2.22)$$

Eq. 2.23 defines an infinite number of discrete characteristic values of the product $k_n d$ for each value of $\frac{\sigma^2 d}{g}$ or $\frac{d}{gT^2}$. The parameter $\frac{d}{gT^2}$ is one of the fundamental dimensionless parameters associated with periodic wave theory. Note that for any value of the subscript n the corresponding value of $k_n d$ must be such that

$$(2n-1) \frac{\pi}{2} \leq k_n d \leq n\pi \quad (2.24)$$

and that for large values of n ,

$$k_n d \approx n\pi \quad (2.25)$$

Also, associated with each value of $k_n d$ is a characteristic shape, viz $\cos [k_n z] = \cos [(k_n d) (\frac{z}{d})]$.

The standing wave nature of Φ_s can be illustrated readily by examining the product of the spatial and temporal terms for large values of the radial distance which is as follows.

$$K_m [k_n r] \exp[-i\sigma t] \approx \sqrt{\frac{\pi}{2k_n r}} \exp[-k_n r] \exp[-i\sigma t] \quad (2.26)$$

Eq. 2.26 satisfies the basic idea of a standing wave of amplitude diminishing with increasing distance from the center.

The unknown coefficients A_n and $B_{m,n}$ in the outgoing and standing wave potentials, may be determined by use of the orthogonality relationships and the boundary condition at the rod. The orthogonality relationships are summarized as follows.

$$\int_0^d \cos [k_n d] \cosh [kz] dz = 0 \quad (2.27)$$

$$\int_0^d \cos [k_n d] \cos [k_m d] dz = \begin{cases} 0 & \text{if } n \neq m \quad (2.28a) \\ \frac{\{k_n d + \sin[k_n d] \cos [k_n d]\}}{k_n} & \text{if } n=m \quad (2.28b) \end{cases}$$

In the following work it will prove useful to have succinct definitions for certain integral terms. Accordingly, the following definitions are made.

$$\begin{aligned}
I_1[k_n d] &= \frac{1}{d} \int_0^d \left(\frac{z}{d}\right) \cos [k_n z] dz \\
&= \left(\frac{1}{k_n d}\right)^2 (k_n d \sin [k_n d] + \cos [k_n d] - 1)
\end{aligned} \tag{2.29}$$

$$I_2[k_n d] = \frac{1}{d} \int_0^d \cos^2 [k_n z] dz = \frac{1}{2k_n d} (k_n d + \sin [k_n d] \cos [k_n d]) \tag{2.30}$$

$$\begin{aligned}
I_3[kd] &= \frac{1}{d} \int_0^d \left(\frac{z}{d}\right) \cosh [kz] dz \\
&= \left(\frac{1}{kd}\right)^2 (kd \sinh [kd] - \cosh [kd] + 1)
\end{aligned} \tag{2.31}$$

$$I_4[kd] = \frac{1}{d} \int_0^d \cosh^2 [kz] dz = \frac{1}{2kd} (kd + \sinh [kd] \cosh [kd]) \tag{2.32}$$

where the dependence of the result is emphasized by the bracketed term, i.e., $[k_n d]$.

2.5 EVALUATION OF COEFFICIENTS $B_{m,n}$ AND C_n

In order to evaluate the unknown coefficients $B_{m,n}$ and C_n , the remaining boundary condition at the rod, condition (c) in section 2.4, must be satisfied with the aid of the orthogonality relations given in Eq. 2.27 and 2.28. Suppose that the angular response displacement, velocity, and acceleration of the rod is given by the real part of the following expressions.

$$\alpha = A \exp [-i\sigma t] \tag{2.33}$$

$$\dot{\alpha} = -i\sigma A \exp [-i\sigma t] \tag{2.34}$$

$$\ddot{\alpha} = +i^2 \sigma^2 A \exp [-i\sigma t] \tag{2.35}$$

where A is the complex amplitude of the response. Accordingly, for small displacements, the radial fluid particle velocity must be as follows

$$-\frac{\partial \Phi}{\partial r} [R, \theta, z, t] = -i\sigma A d \left(\frac{z}{d}\right) \cos [\theta] \exp [-i\sigma t] \quad (2.36)$$

where the derivative of Φ is evaluated at the surface of the cylinder, i.e., at $r = R$. In order to determine each set of coefficients separately, multiply Eq. 2.36 by $\cos [k_j z]$ and integrate over the water column. Thus

$$\begin{aligned} \int_0^d \left(\frac{\partial \Phi_i}{\partial r} + \frac{\partial \Phi_o}{\partial r} + \frac{\partial \Phi_s}{\partial r} \right) \cos [k_n z] dz \\ = i\sigma A d \cos [\theta] \exp [-i\sigma t] \int_0^d \frac{z}{d} \cos [k_n z] dz \quad (2.37) \end{aligned}$$

Because of Eqs. 2.27 and 2.28, Eq. 2.37 becomes

$$\sum_{m=0}^{\infty} B_{m,j} k_j K'_m [k_j R] \cos [m\theta] I_2 [k_j d] = i\sigma d^2 A I_1 [k_j d] \cos [\theta] \quad (2.38)$$

Accordingly, $B_{m,j}$ is as follows

$$B_{1,j} = \frac{i\sigma d A I_1 [k_j d]}{k_j K'_1 [k_j R] I_2 [k_j d]} \quad (2.39a)$$

$$B_{mj} = 0 \quad \text{if } m \neq 1 \quad (2.39b)$$

where K'_m is the derivative of K_m with respect to the argument $k_j r$. Since only the case $m = 1$ is of interest, the potential function for the standing wave can be simplified as follows.

$$\phi_s = \sum_{n=1}^{\infty} B_n K_1[k_n r] \cos[k_n z] \cos[\theta] \exp[-i\sigma t] \quad (2.40)$$

where

$$B_n = \frac{i\sigma d A I_1[k_n d]}{k_n K_1'[k_n R] I_2[k_n d]} \quad (2.41)$$

In order to find C_n , multiply Eq. 2.36 by $\cosh[kz]$ and integrate over the water column. Accordingly,

$$\begin{aligned} & \int_0^d \left\{ \frac{\partial \phi_i}{\partial r} + \frac{\partial \phi_o}{\partial r} \right\} \cosh[kz] dz \\ &= i\sigma A d \cos[\theta] \exp[-i\sigma t] \int_0^d \frac{z}{d} \cosh[kz] dz \quad (2.42) \end{aligned}$$

The left hand side of Eq. 2.42 becomes

$$\begin{aligned} & k A_1 d I_4[kd] \{ J_0'[kR] + 2 \sum_{n=1}^{\infty} i^n J_n'[kR] \cos[n\theta] \} \\ &+ \sum_{n=0}^{\infty} C_n k H_n^{(1)'}[kR] \cos[n\theta] d I_4[kd] \end{aligned}$$

where $H_n^{(1)'}[kR]$ means the derivative of $H_n^{(1)}$ with respect to kr evaluated at $r = R$, and similarly for $J_n'[kR]$. The right hand side becomes $i\sigma A d^2 \cos[\theta] I_3[kd]$.

Accordingly,

$$C_0 = \frac{-A_1 J_0'[kR]}{H_0^{(1)'}[kR]} \quad (2.43a)$$

$$C_1 = \frac{-2iA_1 J_1' [kR]}{H_1 (1)' [kR]} + \frac{i\sigma Ad I_3 [kd]}{kH_1 (1)' [kR] I_4 [kd]} \quad (2.43b)$$

$$C_n = \frac{-2A_1 i^n J_n' [kR]}{H_n (1)' [kR]} \quad \text{for } n \geq 2 \quad (2.43c)$$

Note that except for the last part of the coefficient C_1 , the coefficients C_n are independent of the motion of the rod. In fact, except for the second part of C_1 , the coefficients are identical to those which are obtained by assuming the rod to be at rest always. This suggests that the influence of the outgoing wave be separated into two parts: viz, one part describing the static solution, and one part defined by the motion of the rod. Thus

$$\Phi_o = \Phi_o' + \Phi_o'' \quad (2.44)$$

where Φ_o' is associated with the static part of the solution and Φ_o'' is the part associated with the rod motion.

2.6 SUMMARY OF THE SOLUTION

The solution of the problem may now be summarized. The total complex velocity potential, Φ , is

$$\Phi = (\Phi_i + \Phi_o') + (\Phi_o'' + \Phi_s) \quad (2.45)$$

where Φ_i is the incident wave potential, Φ_o' and Φ_o'' are the two parts of the radiated wave potential and Φ_s is the standing wave potential. The following physical interpretation is useful. The forces associated with the term

$(\phi_i + \phi'_0)$ are the forces which would act on a pile at rest loaded by the incident waves. The forces associated with the second term, $(\phi''_0 + \phi_s)$ are produced by the motion of the structure: that is, they may be interpreted eventually as producing the "added mass" and "radiation damping". The pertinent equations are as follows:

$$\phi_i = A_i \cosh [kz] \{ J_0[kr] + 2 \sum_{n=1}^{\infty} i^n J_n[kr] \cos [n\theta] \} \exp[-i\sigma t] \quad (2.46)$$

$$\phi'_0 = \sum_{n=0}^{\infty} C'_n H_n^{(1)}[kr] \cos [n\theta] \cosh [kz] \exp[-i\sigma t] \quad (2.47)$$

$$\phi''_0 = C''_1 H_1^{(1)}[kr] \cos [\theta] \cosh [kz] \exp[-i\sigma t] \quad (2.48)$$

$$\phi_s = \sum_{n=1}^{\infty} B_n K_1[k_n r] \cos [\theta] \cos [k_n z] \exp[-i\sigma t] \quad (2.49)$$

where

$$A_i = \frac{ag}{\sigma \cosh [kd]} \quad (2.50)$$

$$C'_0 = \frac{-A_i J'_0[kR]}{H'_0[kR]} \quad (2.51)$$

$$C'_n = \frac{-2i^n A_i J'_n[kR]}{H_n^{(1)'}[kR]}, \quad n \geq 1 \quad (2.52)$$

$$C''_1 = \frac{i\sigma A_i I_3[kd]}{k H_1^{(1)'}[kR] I_4[kd]} \quad (2.53)$$

$$B_n = \frac{i\sigma d A I_1[k_n d]}{k_n K_1'[k_n R] I_2[k_n d]} \quad (2.54)$$

$$\sigma^2 = gk \tanh[kd] \quad (2.55)$$

$$\sigma^2 = -gk_n \tan[k_n d] \quad (2.56)$$

$$I_1[k_n d] = \frac{1}{(k_n d)^2} (k_n d \sin[k_n d] + \cos[k_n d] - 1) \quad (2.57)$$

$$I_2[k_n d] = \frac{1}{2k_n d} (k_n d + \sin[k_n d] \cos[k_n d]) \quad (2.58)$$

$$I_3[kd] = \frac{1}{(kd)^2} (kd \sinh[kd] - \cosh[kd] + 1) \quad (2.59)$$

$$I_4[kd] = \frac{1}{2kd} (kd + \sinh[kd] \cosh[kd]) \quad (2.60)$$

In computing results it is occasionally convenient to rewrite the last four equations given above in alternate forms. Some of these forms may be summarized as follows

$$I_1[k_n d] = \frac{(\frac{\sigma_d^2}{g} - 1) \sin[k_n d]}{\frac{\sigma_d^2}{g} (k_n d)} - \frac{1}{(k_n d)^2} \quad (2.61)$$

$$I_1[k_n d] = \frac{1}{(k_n d)^2} \{(-\frac{\sigma_d^2}{g} + 1) \cos[k_n d] - 1\} \quad (2.62)$$

$$I_2[k_n d] = \frac{1}{2} (1 - \frac{\sin^2[k_n d]}{\frac{\sigma_d^2}{g}}) \quad (2.63)$$

$$I_3[kd] = \frac{\left(\frac{\sigma_d^2}{g} - 1\right) \sinh[kd]}{kd \left(\frac{\sigma_d^2}{g}\right)} + \frac{1}{(kd)^2} \quad (2.64)$$

$$I_3[kd] = \frac{1}{(kd)^2} \left\{ \left(\frac{\sigma_d^2}{g} - 1\right) \cosh[kd] + 1 \right\} \quad (2.65)$$

$$I_4[kd] = \frac{1}{2} \left(1 + \frac{\sigma_d^2}{g} \frac{\cosh^2[kd]}{kd} \right) \quad (2.66)$$

$$I_4[kd] = \frac{1}{2} \left(1 + \frac{\sinh^2[kd]}{\frac{\sigma_d^2}{g}} \right) \quad (2.67)$$

In Chapter 3, these equations will be used to examine the ideal fluid forces on static structures. In Chapter 4, they are used to examine the forces associated with dynamic structural response.

CHAPTER 3

FORCES ACTING ON A STATIC STRUCTURE

3.1 INTRODUCTION

This chapter discusses the hydrodynamic forces associated with the interaction of a harmonic wave and a cylindrical member. The member is the cylinder shown in Fig. 1.1 except that its base is attached to the foundation in a rigid fashion. Accordingly, the cylinder responds in a static manner to the wave forces. McCamy and Fuchs (6) first presented the solution for hydrodynamic forces associated with this static problem.

The solution presented here agrees with theirs when expressed in similar terms. Several approximations of interest are also presented in the following discussion.

3.2 STATIC FORCES

As noted in Sec. 2.6, the forces associated with the potential terms $(\phi_1 + \phi'_0)$ are those that would act on a pile at rest and loaded by the incident wave. The force intensity of force per unit length, f_o , on a circular cylinder of radius may be computed with the aid of Eq. 2.14 and Eq. 2.45(a) and 2.45(b) as follows.

$$f_o = 2i\sigma\rho R \int_0^\pi (\phi_1 + \phi'_0) \cos [\theta] d\theta \quad (3.1)$$

$$f_o = \frac{-4A_1\rho\sigma}{k} \frac{\cosh [kz] e^{-i(\sigma t - v)}}{\sqrt{(J'_1[kR])^2 + (Y'_1[kR])^2}} \quad (3.2)$$

where

$$v = \tan^{-1} \left[\frac{J'_1[kR]}{Y'_1[kR]} \right] \quad (3.3)$$

A_i is the incident wave coefficient defined by Eq. 2.50. The quantities $J_1'[kR]$ and $Y_1'[kR]$ are the derivatives of the Bessel function, $dJ_1[kR]/d(kr)$ and $dY_1[kR]/d(kr)$, evaluated at kR . Recall that the local particle acceleration in the incident wave at $r = 0$ or $x = 0$ is

$$\frac{\partial u}{\partial t} = \frac{-\partial^2 \Phi}{\partial x \partial t} = -A_i k \sigma \cosh[kz] e^{-i\sigma t} \quad (3.4)$$

$$= \left(\frac{\partial u}{\partial t} \right)_{\max} e^{-i\sigma t} \quad (3.5)$$

so that $(\partial u / \partial t)_{\max} = -A_i k \sigma \cosh[kz]$. Now let

$$C_I = \frac{4}{\pi (kR)^2 \sqrt{(J_1'[kR])^2 + (Y_1'[kR])^2}} \quad (3.6)$$

where C_I is the inertia force coefficient.

Accordingly, Eq. 3.2 can be written as follows.

$$f_o = C_I \pi R^2 \rho \left(\frac{\partial u}{\partial t} \right)_{\max} \cos [\sigma t - \nu] \quad (3.7)$$

Thus, the force intensity at any point along the pile is proportional to the ambient local water particle acceleration. However, the force intensity lags the wave acceleration by the angle ν . The proportionality factor is equal to the mass of fluid displaced per unit length by the pile multiplied by a coefficient of inertia, C_I .

The relationship between the inertia coefficient and ratio of cylinder diameter to wave length, D/λ , is shown in Fig. 3.1. Evidently, if D/λ is less than about 0.2, $C_I \approx 2.0$ within five percent. For large values of D/λ , say $D/\lambda > \sim 0.4$, the following relationship exists.

$$C_I \approx 0.29 \left(\frac{\lambda}{D}\right)^{1.5} \quad \left(\text{if } \frac{\lambda}{D} \geq 0.4\right) \quad (3.8)$$

The inertia coefficient can be determined over entire range of the ratio of cylinder diameter to wave length from the following approximate equation

$$C_I = \frac{2.0}{1.0 + 81.2 \left(\frac{D}{\lambda}\right)^3} + \frac{0.29 \left(\frac{\lambda}{D}\right)^{1.5}}{1 + 0.034 \left(\frac{\lambda}{D}\right)^{3.0}} \quad (3.9)$$

Equation 3.9, which is shown on Fig. 3.1, gives the value of the inertia coefficient to about ± 5 percent for all values of the ratio of cylinder to wave length.

We may evaluate the effect of wave frequency and cylinder diameter on the inertia coefficient in a more useful form by using the relative depth parameter, $\frac{d}{gT^2}$, and the ratio of cylinder diameter to water depth, D/d . Note that the inertia coefficient is essentially equal to 2.0 so long as $d/gT^2 \leq 0.25$ and $D/d \leq 0.1$.

The relationship between the phase angle, ν , and the ratio of cylinder diameter to wave length is given in Fig. 3.3. For ratios of cylinder diameter to wave length less than about 0.6, the inertia force lags the acceleration by as much as 0.355 radians or about 20° ; it lags the acceleration by an increasing amount for larger values of the ratio. For very small values of the ratio of cylinder diameter to wave length, the phase angle, ν , may be computed approximately as

$$\nu \approx \frac{\pi^3}{4} \left(\frac{D}{\lambda}\right)^2 = 7.75 \left(\frac{D}{\lambda}\right)^2 \quad (3.10)$$

This expression is accurate to 5% for values of D/λ less than about 0.15. For values of D/λ larger than about 1.5, the phase angle is given within 5 percent as follows

$$\nu \approx \pi(0.75 - D/\lambda) \quad (3.11)$$

CHAPTER 4

FORCES ASSOCIATED WITH DYNAMIC STRUCTURAL RESPONSE

4.1 INTRODUCTION

The analysis in Chapter 2 shows that the total hydrodynamic pressure resulting from wave-structure interaction can be viewed as consisting of two components: viz, one component which is independent of the structural motion and depends only on wave motion, and one which is independent of wave motion and depends only on structural motion. The component which is independent of structural motion is discussed in Chapter 3. It is identical for structures which respond statically or dynamically. In this chapter, the forces produced solely by structural motion are discussed.

The response-dependent forces may be viewed also as having two components, one is a function of structural velocity and the second a function of structural acceleration. The former is called commonly the "radiation damping" force and the latter is the so-called added mass force. In the following discussion these forces are computed for the simple single degree of freedom system shown in Fig. 1.1. It is assumed that the rod moves in simple harmonic motion. Subsequently, these results are interpreted in terms of more complicated structures.

4.2 SINGLE DEGREE-OF-FREEDOM SYSTEM

According to Eq. 2.45, the potential function associated with angular motion of the rod, $\alpha = A \exp [-i\sigma t]$, is the sum $\phi_o'' + \phi_s$. The force intensity, f_d , acting on the cylinder because of the water may be computed using Eq. 2.14. The result is as follows.

$$f_d = + 2R\rho i\sigma \int_0^\pi (\phi_o'' + \phi_s) \cos[\theta] d\theta \quad (4.1)$$

Thus according to the relationships given in Eqs. 2.48, 2.49, 2.53 and 2.54, the force intensity may be written as follows.

$$f_d = -\pi R\rho\sigma^2 \left\{ \frac{I_3 H_1^{(1)}[kR] \cosh[kz]}{k H_1^{(1)'}[kR] I_4} + \sum_{n=1}^{\infty} \frac{I_1 K_1[k_n R] \cos[k_n z]}{k_n K_1'[k_n R] I_2} \right\} A \exp[-i\sigma t] \quad (4.2)$$

The functions I_1, I_2, I_3 , and I_4 are defined in Eqs. 2.57 and 2.60.

It is convenient to write the preceding equation in the following form.

$$f_d = -m_d \{c_r d\dot{\alpha} + c_m d\ddot{\alpha}\} \quad (4.3)$$

The coefficients c_r and c_m may be interpreted as coefficients of "radiation damping intensity" and "added mass intensity". Since $\dot{\alpha}$ and $\ddot{\alpha}$ are the angular velocity and acceleration of the rod, the quantities $d\dot{\alpha}$ and $d\ddot{\alpha}$ represent the linear velocity and acceleration of the rod at the free water surface.

The coefficients in Eq. 4.3 are as follows.

$$c_r = \frac{2\sigma}{\pi(kR)^2 \{ (J_1'[kR])^2 + (Y_1'[kR])^2 \}} \frac{I_3}{I_4} \cosh[kz] \quad (4.4)$$

$$c_m = - \frac{J_1[kR]J_1'[kR] + Y_1[kR]Y_1'[kR]}{kR\{(J_1'[kR])^2 + (Y_1'[kR])^2\}} \frac{I_3}{I_4} \cosh kz$$

$$- \sum_{n=1}^{\infty} \frac{K_1[kR]}{k_n R K_1'[kR]} \frac{I_1}{I_2} \cos [k_n z] \quad (4.5)$$

The force intensity may be integrated to produce total hydrodynamic force, F , where

$$F = \int_0^d f dz = -M_d \{C_r d\dot{\alpha} + C_m d\ddot{\alpha}\} \quad (4.6)$$

M_d is the total mass of water displaced by the rod, and the radiation damping coefficient, C_r , and the added mass coefficient, C_m , are defined as follows.

$$C_r = \frac{1}{d} \int_0^d c_r dz \quad (4.7)$$

$$C_m = \frac{1}{d} \int_0^d c_m dz \quad (4.8)$$

4.3 RADIATION DAMPING FORCE

According to Eq. 4.6 the total radiation damping force is $M_d C_r (d\dot{\alpha})$, i.e., the product of the displaced mass, the radiation damping coefficient, and velocity. The radiation damping coefficient depends only on the relative depth parameter, d/gT^2 , and the ratio of the cylinder radius, R , to the water depth, d . This relationship is shown in Fig. 4.1. For fixed values of the ratio R/d , the radiation damping coefficient increases from zero to a maximum, and decreases to zero as d/gT^2 increases from zero to infinity. The location of the maximum value of C_r as well as its magnitude are dependent on the radius to depth ratio.

According to Eq. 4.4, the distribution of the damping force intensity is proportional to $\cosh[kz]$. Accordingly, the location of the centroid of the intensity distribution, \bar{z} , above the seabed is

$$\bar{z} = \left\{ \int_0^d z \cosh[kz] dz \right\} / \left\{ \int_0^d \cosh[kz] dz \right\}.$$

The relationship between \bar{z}/d and the relative depth parameter, d/gT^2 , is shown in Fig. 4.2. For small values of the relative depth parameter, $\bar{z}/d \sim 0.5$, i.e., the force acts at the middle of the water column. For large values, the force acts near the free water surface since \bar{z}/d approaches 1.0 as noted by Petrauskus (6).

It is useful to separate the various factors in the radiation damping coefficient and write it in the following form.

$$C_r = \sigma C_r' C_r'' \quad (4.9)$$

$$C_r' = \frac{2}{\pi(kR)^2 \{ (J_1' [kR])^2 + (Y_1' [kR])^2 \}} \quad (4.10)$$

$$C_r'' = \frac{I_3}{I_4} \frac{\sinh[kd]}{kd} \quad (4.11)$$

This separates the coefficient into three parts: viz, (1) the circular frequency, (2) a factor (C_r') dependent upon the ratio of cylinder diameter to wave length ($kR=\pi D/\lambda$), and (3) a factor (C_r'') dependent upon d/gT^2 and the mode shape or displacement pattern of the structure.

Figure 4.3 shows the relationship between C_r' and the ratio of cylinder diameter to generated wave length, D/λ . Recall that $\lambda=2\pi/k$ and the wave number is related to frequency by the relationship $\sigma^2=gk \tanh[kd]$ as noted in Eq. 2.3. For increasing values of D/λ , C_r' increases from zero to a maximum value of 0.74 at $D/\lambda = 0.32$; thereafter C_r' diminishes and approaches zero as D/λ grows large. The relationship shown in the figure

may be approximated easily for both large and small values of D/λ as follows.

$$C'_R \sim \frac{\pi}{2} (D/\lambda)^2 \quad (4.12)$$

$$C'_R \sim \frac{1}{\pi} (D/\lambda)^{-1} \quad (4.13)$$

Eq. 4.12 is in error less than 5 percent for $D/\lambda \leq 0.17$, Eq. 4.13 is in error less than 5 percent for $D/\lambda \geq 0.50$. For all values of D/λ , C'_R may be approximated as follows.

$$C'_R = \frac{1.13 \left(\frac{\lambda/D}{0.27}\right)^3}{1 + 2.7 \left(\frac{\lambda/D}{0.27}\right)^5} + \frac{1.18 \left(\frac{0.27}{\lambda/D}\right)}{1 + 2.2 \left(\frac{0.27}{\lambda/D}\right)^5} \quad (4.14)$$

This equation is shown as the "approximate" solution on Fig. 4.3.

For a specific mode shape (in this case the "triangular" one z/d) the second parameter, C''_r , depends only on d/gT^2 . The relationship between C''_r and d/gT^2 is shown on Fig. 4.4. For values of d/gT^2 less than about 0.6, $C''_r \sim 0.5$. For large values of relative depth

$$C''_r \sim 0.05 \left(\frac{d}{gT^2}\right)^{-1} \quad (4.15)$$

4.4 ADDED MASS FORCE

According to Eq. 4.6 the total added mass force is $M_d C_m (d\ddot{x})$, i.e., the product of the displaced mass, the added mass coefficient, and acceleration. The added mass coefficient depends on the ratio of the cylinder diameter to

water depth, D/d , and the relative depth parameter, d/gT^2 , i.e.,
 $C_m = C_m [D/d, d/gT^2]$. This relationship is shown in Fig. 4.5 for the hinged rod. According to two-dimensional ideal fluid theory, the added mass intensity force of a cylinder is 1.0 times the mass of water displaced times the acceleration. If this two-dimensional model were used to compute the added mass coefficient for the present problem, the result would be $C_m = 0.5$ since the acceleration used in Eq. 4.6 is that at the top of the rod.

According to Fig. 4.5, the added mass coefficient approaches a value of 0.5 as the relative depth parameter approaches zero. For increasing values of relative depth parameter, the coefficient increases to a maximum slightly above the 0.5 value and then decreases to a minimum which is dependent strongly on the ratio of cylinder diameter to depth. For still larger values of the relative depth parameter the coefficient increases and approaches an asymptotic value as d/gT^2 approaches infinity. For small values of the ratio of cylinder diameter to depth, the added mass coefficient deviates only slightly from the equivalent two dimensional value. For example, if D/d is 0.1 the added mass coefficient has a maximum value of 0.52 and a minimum value of 0.45 at d/gT^2 equals infinity.

Fig. 4.6 shows the relationship between the ratio of the added mass force moment arm to water depth, \bar{z}_m/d , and the relative depth parameter for various ratios of cylinder diameter to water depth. Since the mode shape is triangular the equivalent two-dimensional result would be $\bar{z}_m/d = 0.67$. The moment arm parameter is strongly dependent upon the ratio D/d for large values of relative depth parameter.

Fig. 4.7 shows the relationship between the added mass intensity coefficient, c_m , and the dimensionless depth, z/d , for a cylinder diameter to water depth ratio of $D/d = 0.10$ and various values of the relative depth parameter, d/gT^2 . The figure shows that the added mass intensity varies substantially from that predicted by two-dimensional calculation over the upper quarter of the cylinder. There is also a slight deviation from the two-dimensional results of the seabed. Figs. 4.8 and 4.9 shows similar results for larger diameter cylinders. In these cases the deviation between the two-dimensional solution and the three-dimensional solution is quite marked.

It was noted above that for small values of relative depth parameter, the added mass coefficient approaches the value of 0.5. However the centroidal distance of the added mass force depends upon the ratio D/d . Figure 4.10 shows the relationship between the added mass intensity coefficient, c_m , and the ratio z/d for d/gT^2 is 0.001 and for various values of the ratio D/d . For this very small value of d/gT^2 the deviation between the three-dimensional solution and the two-dimensional solution is quite marked for increasing values of D/d .

On the opposite end of the scale, the added mass again approaches an asymptotic value as d/gT^2 grows large. Fig. 4.11 shows the relationship between the added mass intensity coefficient and the relative depth, z/d , for an infinite value of the relative depth parameter and various values of the ratio D/d .

4.5 FLUID-STRUCTURE INTERACTION FORCES FOR THE TRANSLATIONAL MODE

The preceding analysis pertains to a single degree-of-freedom system in which the deflected shape or "mode" shape, G , of the structure

is restricted to be triangular. However, the assumption of mode shape affects only the two integral terms I_1 and I_3 defined in Eq. 2.29 and 2.30. The results may be generalized to include mode shape by substituting the normalized equation of the mode shape, G , for the quantity z/d in these equations. Of particular interest in the rigid body translational mode, i.e., $G = 1$ for all values of z . The results for this case are shown in Figs. 4.12 to 4.18.

CHAPTER 5

RESPONSE OF OFFSHORE STRUCTURES TO EARTHQUAKES

5.1 INTRODUCTION

The fluid-structure interaction forces determined in the previous chapters may be combined with information pertaining to viscous fluids and structural response spectra to estimate the response of offshore structures to earthquakes. The approach used is somewhat heuristic and is limited to an estimate of response in a single structural mode. They are correct if the base excitation is periodic with frequency equal to the frequency of the structure. The primary purpose for this analysis is to provide an approximate method for investigating the relative importance of these theoretical fluid-structure interaction forces in the response of offshore structures.

The following discussion presents the development of the modal equation of motion for a structure subjected to an earthquake. This equation includes appropriate radiation damping terms which may be evaluated by approximate expressions developed from the equations in the preceding chapters. The radiation damping terms enter into the modal equation in different fashion than viscous damping appears in the equation of motion used as a basis for the structural response spectrum in earthquake engineering. The effect of the radiation damping terms on the response spectrum is described.

5.2 MODAL EQUATIONS OF MOTION

Suppose the single degree-of-freedom (SDF) system shown in Fig. 5.1(a) is subjected to a time-dependent base acceleration, \ddot{x}_0 . If the relative motion coordinate $x = x_s - x_0$ is adopted where x_s is the absolute displacement of the mass, the equation of motion for the system is

$$\ddot{x} + 2\beta\omega\dot{x} + \omega^2 x = -\ddot{x}_0 \quad (5.1)$$

The undamped circular natural frequency is ω and β is the damping ratio associated with structural damping. The quantities \dot{x} and \ddot{x} are the relative velocity and acceleration respectively. The general solution of this equation is

$$x = -\frac{1}{\omega_d} \int_0^t \ddot{x}_0 \exp[-\beta\omega(t-\tau)] \sin[\omega_d(t-\tau)] d\tau \quad (5.2)$$

where ω_d is the damped circular frequency. By convention, the structural response spectrum is a plot of psuedo-velocity, V , as a function of the natural frequency f_s ($f_s = \omega/2\pi$), or period T_s ($T_s = 1/f_s$) where the psuedo-velocity is $V = \omega |x_{\max}|$ and x_{\max} is maximum value of displacement given by Eq. 5.2. Thus, the response spectrum depends only upon the damping β , and the nature of the base acceleration, \ddot{x}_0 . Figure 5.2 is a sketch of an idealized structural response spectrum. Such spectra may be readily constructed from a knowledge of the maximum ground displacement, velocity, and acceleration using empirical methods (10).

Now consider a structure similar to that shown in Fig. 5.1(b) except that it is surrounded by air rather than water shown in the figure. The structure may have any number of degrees of freedom. In the case of multi-degree-of-freedom systems, the analysis is greatly simplified by using the normal mode method (10). This permits the set of equations of motion which are coupled usually to be written in uncoupled form as a set of simple equations, each one of which represents the response of a single mode of the system. For example, suppose for relative motion, x , of the structure shown in Fig. 5.1(b) is written in terms of the normal modes, i.e., $x = \sum \zeta_{ai} q_i$, where ζ_{ai} is the mode shape of the i^{th} mode when the structure is in air and q_i is the associated generalized displacement coordinate which is a function of

time; the summation extends over all modes. Then the i^{th} modal equation is

$$\ddot{q}_i + 2\beta_{ai}\omega_{ai}\dot{q}_i + \omega_{ai}^2 q_i = -\Gamma_{ai}\ddot{x}_o \quad (5.3)$$

where \dot{q} and q are the modal velocity and displacement respectively. The damping ratio in air is β_{ai} , and ω_{ai} is the natural frequency in air. The quantity Γ_{ai} is the participation factor of the i^{th} mode in air and is computed as follows.

$$\Gamma_{ai} = \frac{\int m\zeta_{ai} dz}{M_{ai}^*} \quad (5.4)$$

The modal mass M_{ai}^* in air is

$$M_{ai}^* = \int m\zeta_{ai}^2 dz \quad (5.5)$$

where m is the mass per unit length of the structure. In the two preceding equations the integration is carried out over the entire length of the structure. It is clear that the maximum value of the modal structural response is Γ_{ai} times the response determined from the response spectrum such as Fig. 5.2.

How does the surrounding water envelope modify the modal equation, Eq. 5.2, according to ideal fluid theory? First, we must define the natural frequency and mode shape in water as ω_{wi} and ζ_{wi} . Obviously, the modal value of the fluid-structure interaction force, $\int_0^d f\zeta_{wi} dz$, must be incorporated in the right hand side of Eq. 5.3. The quantity f is the force intensity, i.e., force per unit length, produced by the motion of the structure through the water. This force intensity may be determined from the analysis given in the preceding chapters if one assumes the fluid to be inviscid, the structure to be modeled by a circular cylinder, and only

a single mode participating in the solution. Then, generalizing Eq. 4.3, it is as follows

$$f = -m_d \{ \sigma C_R \dot{q} + C_M \ddot{q} \} \quad (5.6)$$

where m_d is mass of water displaced per unit length of structure. The coefficients C_R and C_M must be revised to include the translational as well as modal component of relative displacement as shown in Fig. 5.1. Thus the coefficients C_1'' and B_n in Eq. 2.48 and 2.49, respectively, must be found such that the radial velocity at the cylinder wall ($r = R$) is $(\dot{x}_o + \zeta_{wi} \dot{q}) \cos[\theta]$. The result is as follows.

$$f = -m_d \sigma \{ C_{R,t} \dot{x}_o + C_{R,i} \dot{q}_i \} - m_d \{ C_{M,t} \ddot{x}_o + C_{M,i} \ddot{q}_i \} \quad (5.7)$$

where

$$C_{R,t} = \frac{I_3'}{I_4'} C_R' \cosh[kz] \quad (5.8a)$$

$$C_{R,i} = \frac{I_3''}{I_4''} C_R' \cosh[kz] \quad (5.8b)$$

$$C_{M,t} = -\frac{I_3'}{I_4'} \left\{ \frac{J_1[kR] J_1'[kR] + Y_1[kR] Y_1'[kR]}{kR (J_1'[kR] J_1'[kR] + Y_1'[kR] Y_1'[kR])} \right\} \cosh[kz] \\ - \sum_{n=1}^{\infty} \frac{K_1[k_n R]}{k_n R K_1'[k_n R]} \cos[k_n z] \frac{I_1'}{I_2} \quad (5.8c)$$

$$C_{M,i} = -\frac{I_3''}{I_4''} \left\{ \frac{J_1[kR] J_1'[kR] + Y_1[kR] Y_1'[kR]}{kR (J_1'[kR] J_1'[kR] + Y_1'[kR] Y_1'[kR])} \right\} \cosh[kz] \\ - \sum_{n=1}^{\infty} \frac{K_1[k_n R]}{k_n R K_1'[k_n R]} \cos[k_n z] \frac{I_1'}{I_2} \quad (5.8d)$$

and

$$I_3' = \frac{1}{d} \int_0^d \cosh[kz] dz \quad (5.9a)$$

$$I_{\zeta i} = \frac{1}{d} \int_0^d \zeta_{wi} \cosh[kz] dz \quad (5.9b)$$

$$I'_1 = \frac{1}{d} \int_0^d \cos[k_n z] dz \quad (5.9c)$$

$$I'_{\zeta i} = \frac{1}{d} \int_0^d \zeta_{wi} \cos[k_n z] dz \quad (5.9d)$$

C'_r is given by Eq. 4.5, and I_2 and I_4 are given by Eq. 2.30 and 2.32, respectively.

In physical terms, Eq. 5.7 indicates the fluid-structure interaction force consists of two radiation damping (i.e. velocity-dependent) terms and two "added mass" terms (i.e. acceleration-dependent). In each case one term is associated with the rigid body or translational mode and the other with the structural mode for relative motion of the structure with respect to the ground. The magnitude of the two radiation damping terms differs according to the differences between $I_{\zeta i}$ and I'_3 . Similarly, the two added mass terms differ according to the differences between I'_1 and $I'_{\zeta i}$.

The radiation damping terms associated with the integral $\int f \zeta_{wi} dz$ may be written using Eq. 5.7 as follows.

$$\dot{x}_o \sigma \int_0^d m_d C_{r,t} \zeta_{wi} dz + \dot{q}_i \sigma \int_0^d m_d C_{ri} \zeta_{wi} dz = \text{L.H.S.}$$

$$\text{R.H.S.} = \sigma C'_r \left\{ \dot{x}_o \frac{I'_3}{I_4} + \dot{q}_i \frac{I'_{\zeta i}}{I_4} \right\} \int_0^d m_d \zeta_{wi} \cosh[kz] dz \quad (5.10)$$

Now define as mass-type term, M_{di} .

$$M_{di} = \int_0^d m_d \zeta_{wi} \cosh[kz] dz \quad (5.11)$$

Then the contribution of the radiation damping terms to the integral

$$\int f \zeta_{wi} dz \text{ is } -\sigma C' M_{di} \{I'_{3o} \ddot{x}_o + I'_{\zeta i} \dot{q}_i\} / I_4.$$

The contribution of the added mass terms in Eq. 5.7 to the integral $\int f \zeta_{wi} dz$ can be written as $-M_t^* \ddot{x}_o - M_{\zeta i}^* \ddot{q}_i$ where

$$M_t^* = \int m_d C_{m,t} \zeta_{wi} dz \quad (5.12)$$

$$M_{\zeta i}^* = \int m_d C_{m,i} \zeta_{wi} dz \quad (5.13)$$

With this nomenclature, the i^{th} modal equation of motion for the structure in water is

$$\ddot{q} + 2(\beta_{wi} + \beta_{r\zeta i}) \omega_{wi} \dot{q}_i + \omega_{wi}^2 q_i = -\Gamma_{wi} \ddot{x}_o - 2\beta_{rti} \omega_{wi} \dot{x}_o \quad (5.14)$$

where β_{wi} , ω_{wi} , and Γ_{wi} are structural damping ratio, i^{th} mode natural frequency, and i^{th} mode participation factor. These quantities are related to the in-air values as follows.

$$\beta_{wi} = \beta_{ai} \left(\frac{M_{ai}^*}{M_{wi}^* + M_{\zeta i}^*} \right) \quad (5.15)$$

M_{wi}^* is the modal mass computed using the mode shape in water.

$$\omega_{wi}^2 = \omega_{ai}^2 \left(\frac{M_{ai}^*}{M_{wi}^* + M_{\zeta i}^*} \right) \quad (5.16)$$

$$\Gamma_{wi} = \frac{M_t^* + \int m \zeta_{wi} dz}{M_t^* + \int m \zeta_{wi}^2 dz} \quad (5.17)$$

That is to say that the modal mass is altered according to the difference between mode shapes in air and water, and increased by the contribution

of the added mass associated with the relative motion of the structure. The mass to be multiplied by the base acceleration is increased by the added mass contribution associated with the rigid body displacement of the structure in the horizontal direction.

The quantities $\beta_{r\zeta i}$ and β_{rti} in Eq. 5.14 are the i^{th} mode radiation damping ratios associated with the relative modal motion and the rigid body motion components respectively. They are given by the following expressions.

$$\beta_{r\zeta i} = \frac{1}{2} C'_r \left(\frac{\sigma}{\omega_{wi}} \right) \left(\frac{I'_{\zeta i}}{I_4} \right) \left(\frac{M_{di}}{M_{ai}^* + M_{\zeta i}^*} \right) \quad (5.18a)$$

$$\beta_{rti} = \frac{1}{2} C'_r \left(\frac{\sigma}{\omega_{wi}} \right) \left(\frac{I'_3}{I_4} \right) \left(\frac{M_{di}}{M_{ai}^* + M_{\zeta i}^*} \right) \quad (5.18b)$$

5.3 APPROXIMATE EXPRESSIONS FOR RADIATION DAMPING

When the relative depth parameter, d/gT^2 , is greater than about 0.08, the expressions for $I'_{\zeta i}/I_4$ and I'_3/I_4 may be approximated in a simple manner. Further, depending on the ratio of cylinder radius to generated wave length, the expression for C'_R may be also approximated in a simple manner. Accordingly, approximate expressions for the radiation damping terms derived in this section may be substituted for Eq. 5.17a and b.

Most of the energy in earthquake ground motion is associated with frequencies greater than about 0.2 Hertz. Then the ratio d/gT^2 will exceed 0.08 for water depths greater than about 65 ft. For values of d/gT^2 in this range, the $\cosh[kz]$ can be taken as $e^{kz}/2$ with very little error. In this situation the radiation damping force is concentrated near the free water surface as pointed out by Petruskas (6). Accordingly, the value of the integral $I'_{\zeta i}$ is not sensitive to

the exact mode shape provided its' values near the free surface are correct. We may, therefore, make at least a rough estimate of the first mode radiation damping using as the mode shape $\zeta_{w1} = z/d$.

First approximate the quantity M_{di} given by Eq. 5.11 as

$$M_{di} = M_d \left\{ \frac{1}{d} \int_0^d \frac{z}{d} \cosh[kz] dz \right\} \quad (5.19a)$$

$$M_{di} = M_d I_3 \quad (5.19b)$$

where M_d is the mass of water displaced by the structure. Let the ratio of this mass to the sum of actual and added mass be defined as λ .

$$\lambda = \frac{M_d}{M_{a1}^* + M_{\zeta 1}^*} \quad (5.20)$$

Then the damping ratios given in Eqs. 5.17 and 5.18 may be written in the following form.

$$\beta_{r\zeta 1} \approx \frac{1}{2} \lambda \left(\frac{\sigma}{\omega_{w1}} \right) C_r' \left(\frac{I_3^2}{I_4} \right) \quad (5.21)$$

$$\beta_{rt1} \approx \frac{1}{2} \lambda \left(\frac{\sigma}{\omega_{w1}} \right) C_r' \left(\frac{I_3 I_3'}{I_4} \right) \quad (5.22)$$

when $d/gT^2 > 0.08$, the integral ratios may be approximated as follows.

$$\frac{I_3^2}{I_4} \approx 2 \frac{\left(1 - \frac{1}{4\pi^2 \frac{d}{gT^2}} \right)^2}{\frac{d}{gT^2}} \quad (5.23)$$

$$\frac{I_3 I_3'}{I_4} \approx 2 \frac{\left(1 - \frac{1}{4\pi^2 \frac{d}{gT^2}} \right)}{\frac{d}{gT^2}} \quad (5.24)$$

The relative unimportance of the mode shape in radiation damping is illustrated in Eqs. 5.23 and 5.24 which are appropriate for the triangular and translational mode shapes. The ratio of the integral terms given in these equations is 0.68 at $d/gT^2 = 0.08$ and approaches 1.0 for larger values of the relative depth parameter. Now using the approximations for C'_r given in Eq. 4.7 and 4.9 the following approximations may be written.

$$\beta_{r\zeta 1} = 2\pi^3 \lambda \left(\frac{\sigma}{\omega_{w1}} \right) \frac{d}{gT^2} \left(1 - \frac{1}{4\pi \left(\frac{d}{gT^2} \right)} \right)^2 \left(\frac{R}{d} \right)^2 \quad \text{if } \frac{R}{gT^2} \leq \sim 0.014 \quad (5.25)$$

$$\beta_{r\zeta 1} = \lambda \frac{\left(1 - \frac{1}{4\pi \frac{d}{gT^2}} \right)^2}{4\pi^2 \frac{d}{gT^2}} \left(\frac{d}{R} \right) \quad \text{if } \frac{R}{gT^2} \geq \sim 0.04 \quad (5.26)$$

For values of R/gT^2 such that $0.014 \leq \frac{R}{gT^2} < 0.04$, the damping terms may be calculated using Eq. 4.10 or Fig. 4.12 to determine C'_r .

CHAPTER 6

SUMMARY

The fluid-structure interaction forces produced by a harmonic surface wave which produces dynamic structural response may be investigated using ideal fluid theory. The theory is deficient in that forces associated with flow separation and other viscous effects are ignored. However, considerable insight into other force characteristics may be gained.

According to potential theory, the forces may be separated into two components: namely one which is independent of the structural response and second component which depends only on structural motion.

According to the results in Chapter 3, the maximum wave force intensity acting on a static cylinder is the product of the inertia coefficient C_I ; the mass of water displaced per unit length of cylinder; and the maximum horizontal particle acceleration. However, this force intensity lags the horizontal fluid particle acceleration by a phase angle, ν . Both ν and C_I may be viewed as functions of the relative depth parameter, d/gT^2 , and the ratio of cylinder diameter to water depth, D/d . These relationships are shown in Figs. 3.2 and 3.4 respectively. For many practical cases of interest, these relationships can be given by approximate expressions. These expressions are also given in Chapter 3.

The forces associated with dynamic structural response are discussed in Chapter 4. These forces may also be considered as having two components; namely (1) the "radiation damping" force, and (2) the "added mass" force.

The total radiation damping force may be written as $-M_d \sigma C_r' C_r'' (d\dot{\alpha})$ where M_d is the mass of water displaced by the cylinder, σ is the frequency

of the cylinder motion and $(d\dot{\alpha})$ is the linear velocity of the cylinder at the free water surface. The coefficient C'_r is a function of the ratio of cylinder diameter to wave length, D/λ , or in alternate form the ratio D/gT^2 . The coefficient C''_r is a function of the relative depth parameter, d/gT^2 , and mode shape or displacement pattern of the cylinder. The spatial distribution of the force intensities which when integrated produce the total radiation damping force is proportional to the $\cosh[kz]/\cosh[kd]$. The wave number is k . The values of C'_r and C''_r are presented in the figures in Chapter 4.

The total added mass force may be written as $-M_d C_m (d\ddot{\alpha})$ where the quantity $(d\ddot{\alpha})$ represents the linear acceleration of the cylinder at the free surface. The added mass coefficient depends upon the ratio of the cylinder diameter to depth, D/d , and the relative depth parameter, d/gT^2 . The spatial distribution of the force intensities which produce the added mass force vary considerably and cannot be expressed in simple form. Computed results for these force intensities as well as for the added mass coefficient are given in the figures which accompany Chapter 4.

Chapter 5 uses the theoretical fluid-structure interaction results to develop approximate values of radiation damping ratios for use in offshore structures subjected to earthquakes. As shown in Chapter 5, there are two radiation terms of interest. One of them is to be multiplied by the modal velocity in the usual way in the equation of motion. The second, however, is to be multiplied by the ground velocity and constitutes an additional force term in the equation of motion. Useful approximations for these two terms are given in Chapter 5.

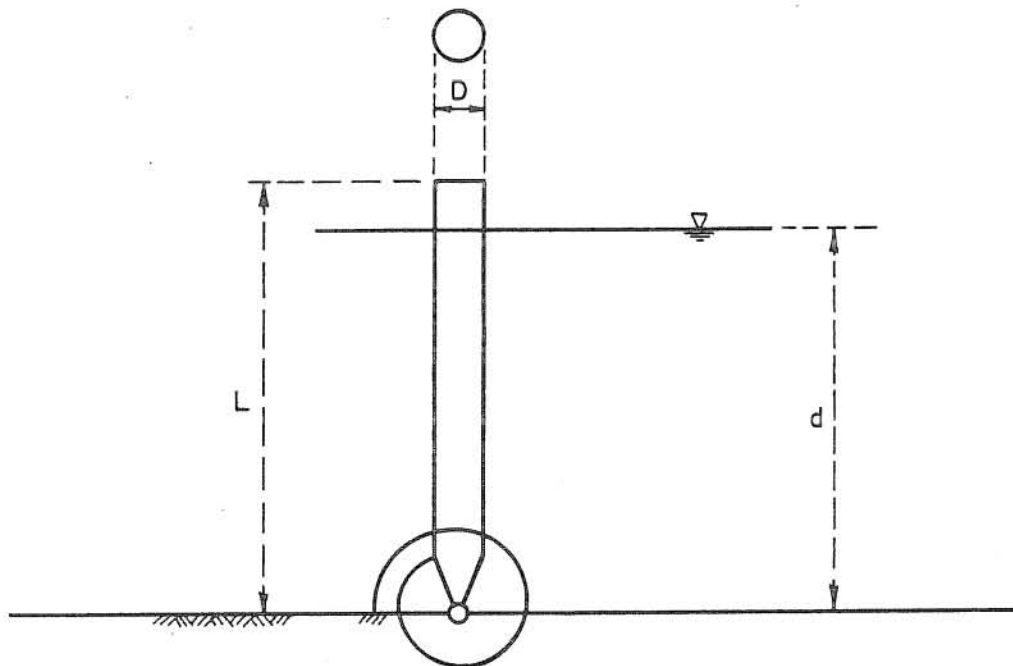


Fig. 1.1 Sketch of a Single Degree-of-Freedom System for Free Surface Fluid Structure Interaction Problems

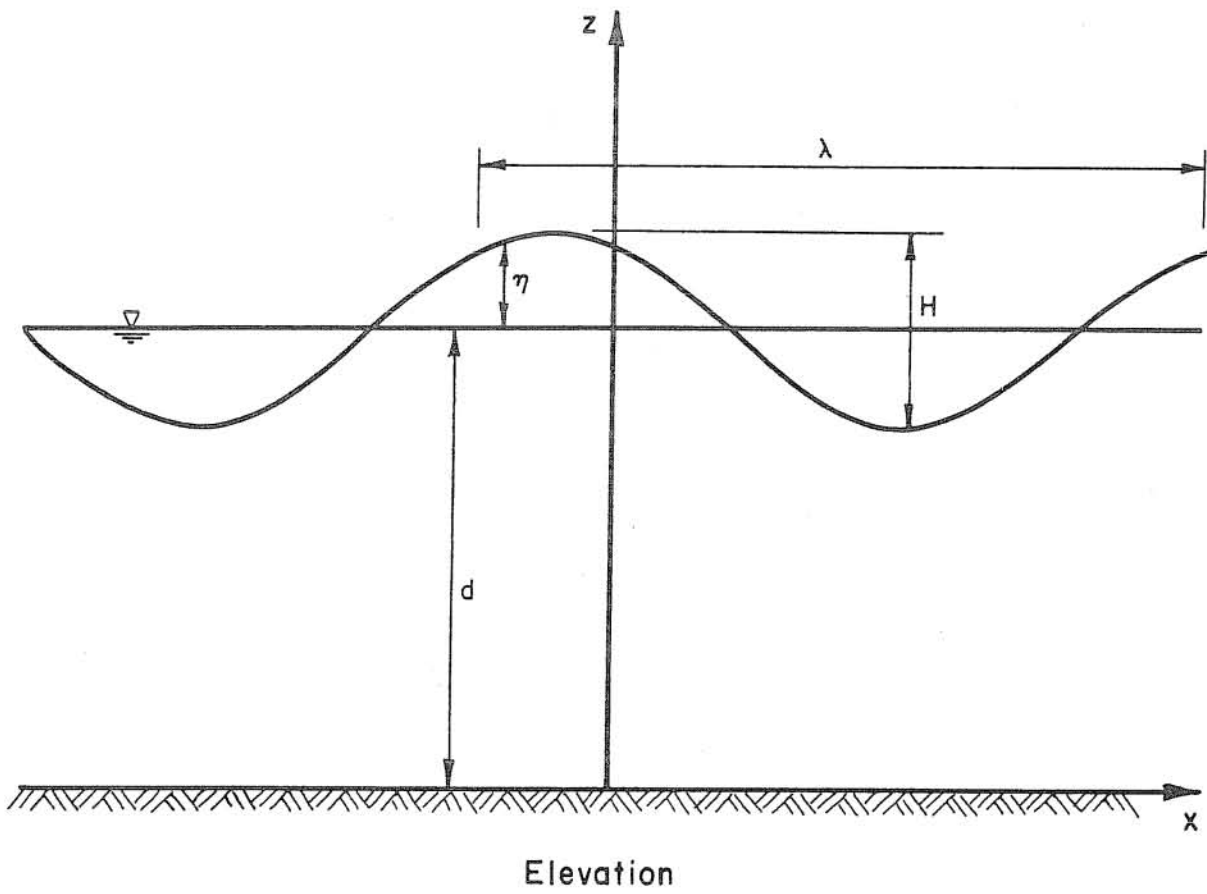
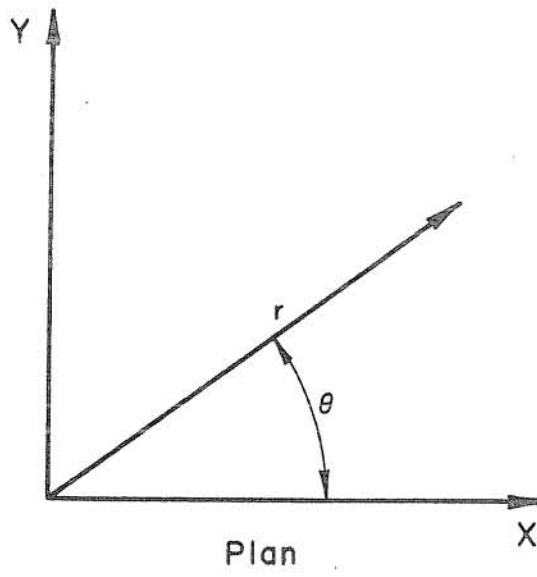


Fig. 1.2 Coordinate Systems

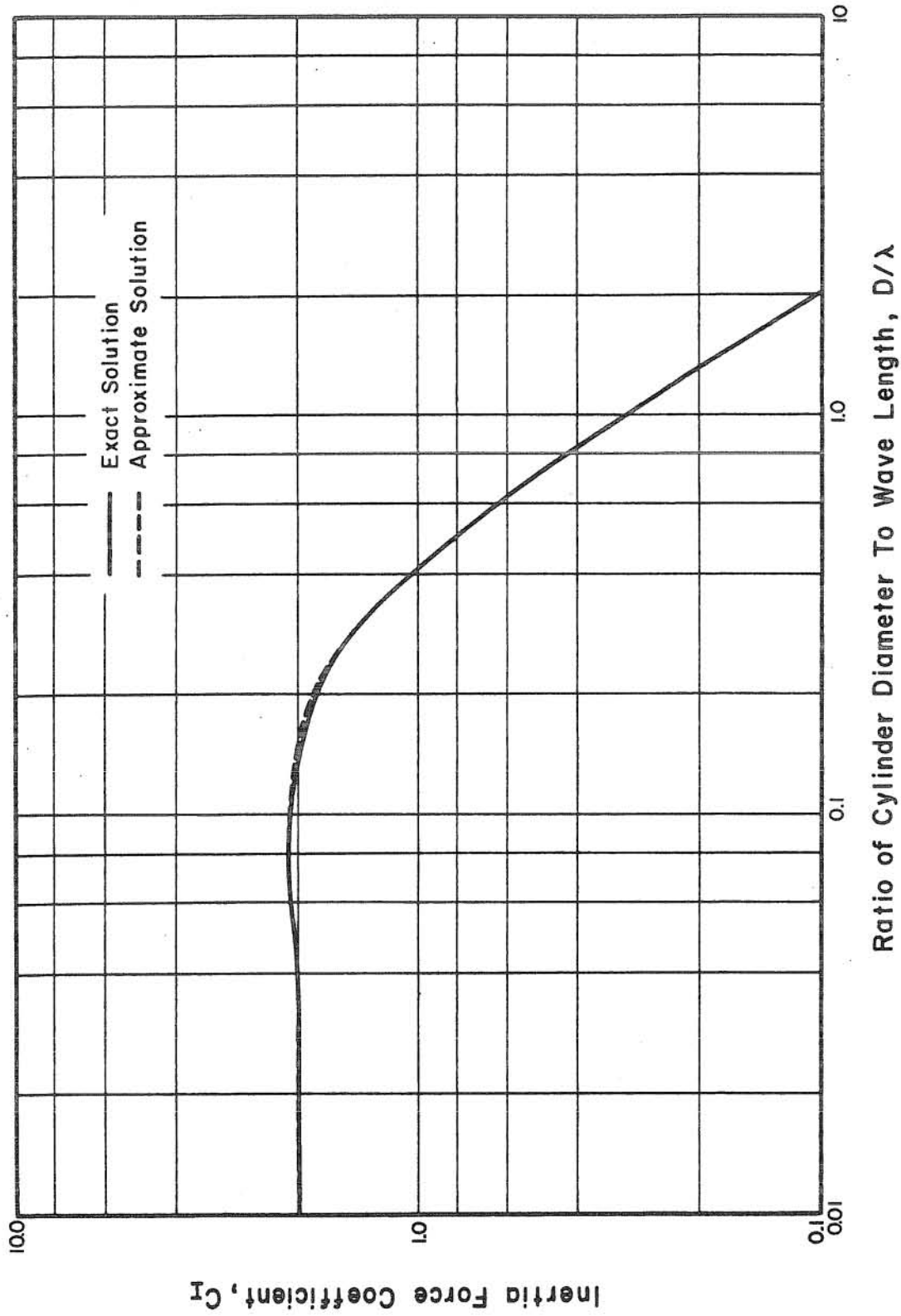


Fig. 3.1 Relationship Between the Inertia Force Coefficient, C_I , and the Ratio of Cylinder Diameter to Wavelength, D/λ .

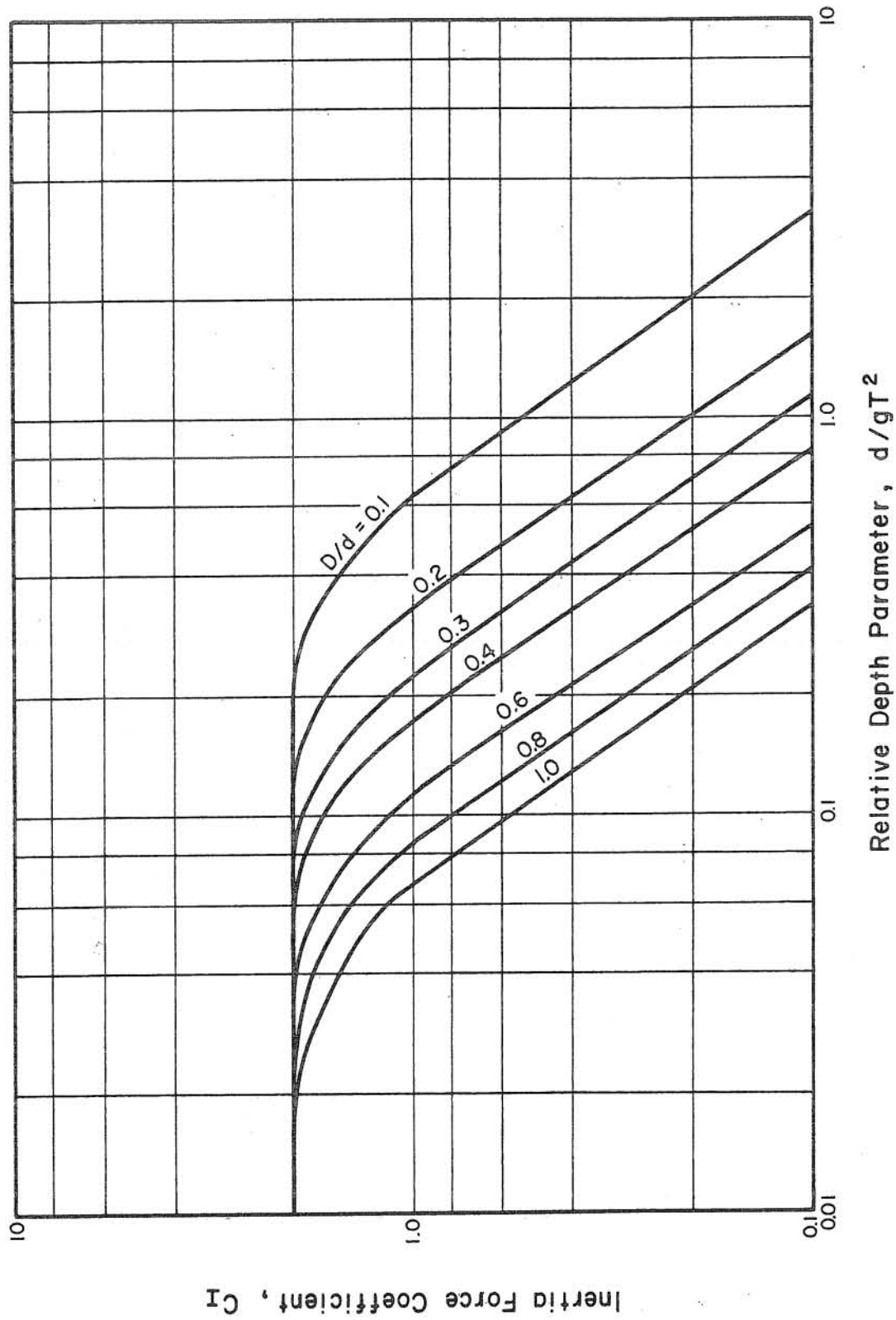


Fig. 3.2 The Relationship Between the Inertia Force Coefficient, C_I , and the Relative Depth, $\frac{d}{gT^2}$, for Various Values of the Ratio of Cylinder Diameter to Water Depth, D/d .

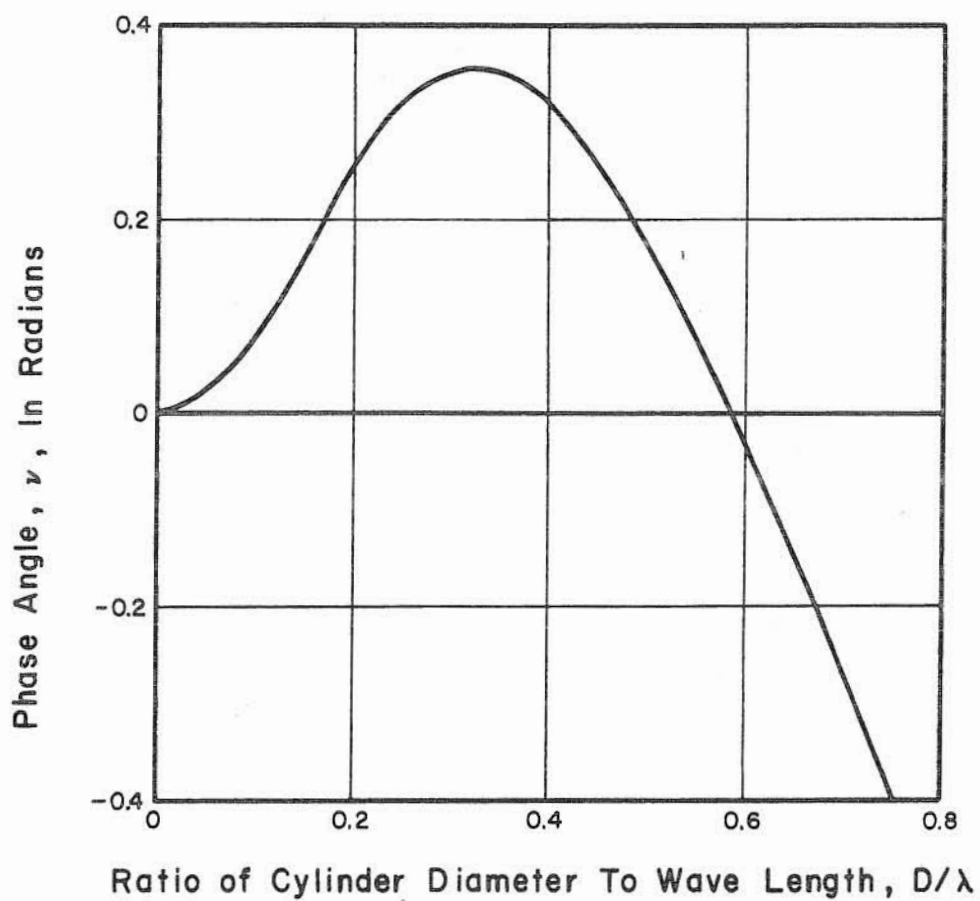


Fig. 3.3 Relationship Between Phase Lag, ν , of the Inertia Force with Respect to the Water Particle Acceleration and the Ratio of Cylinder Diameter to Wave Length, D/λ .

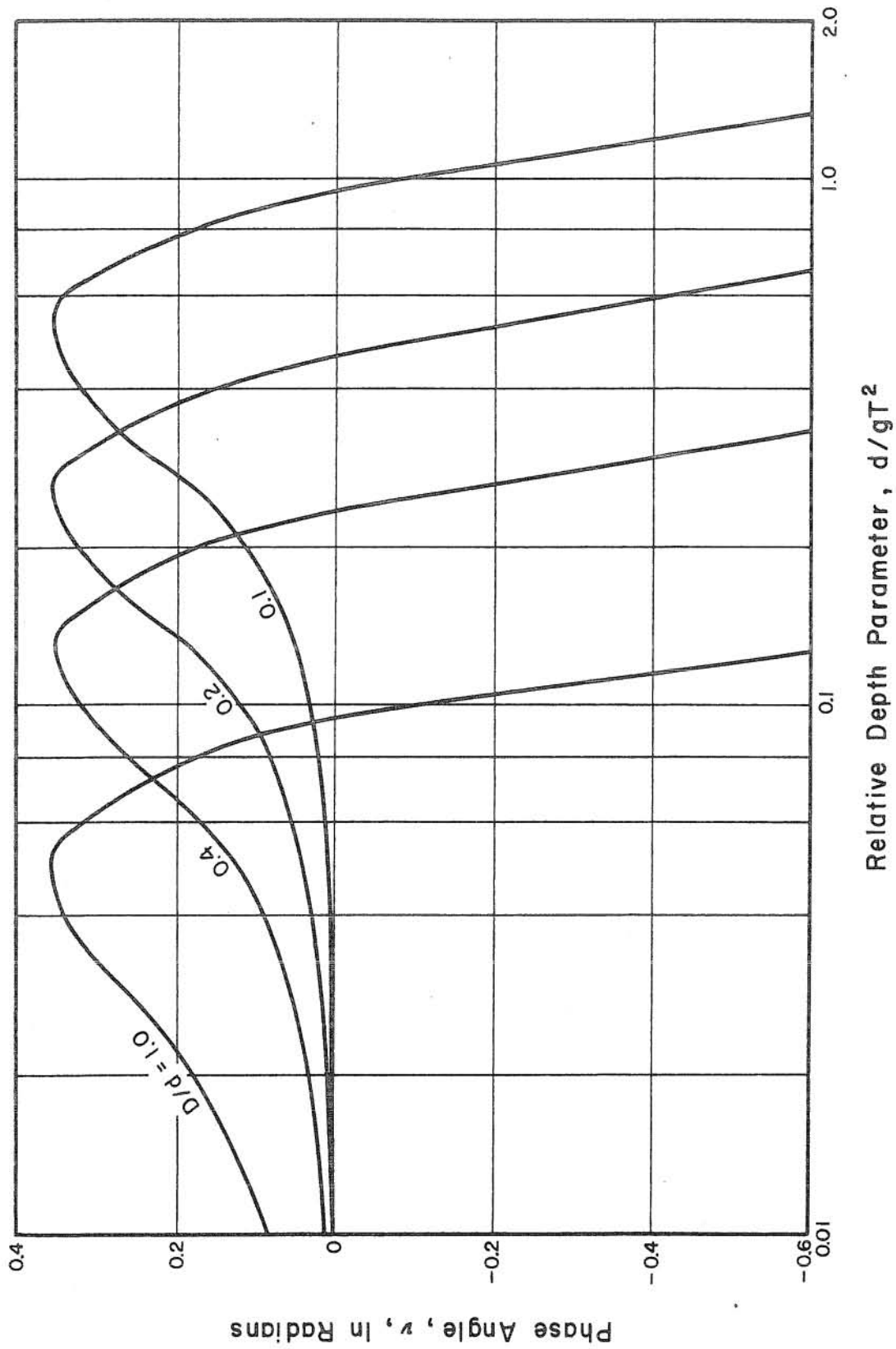


Fig. 3.4 Relationship Between the Phase Lag, ν , of the Inertia Force with Respect to the Water Particle Acceleration and the Relative Depth, d/gT^2 , for Various Values of the Ratio of Cylinder Diameter to Water Depth.

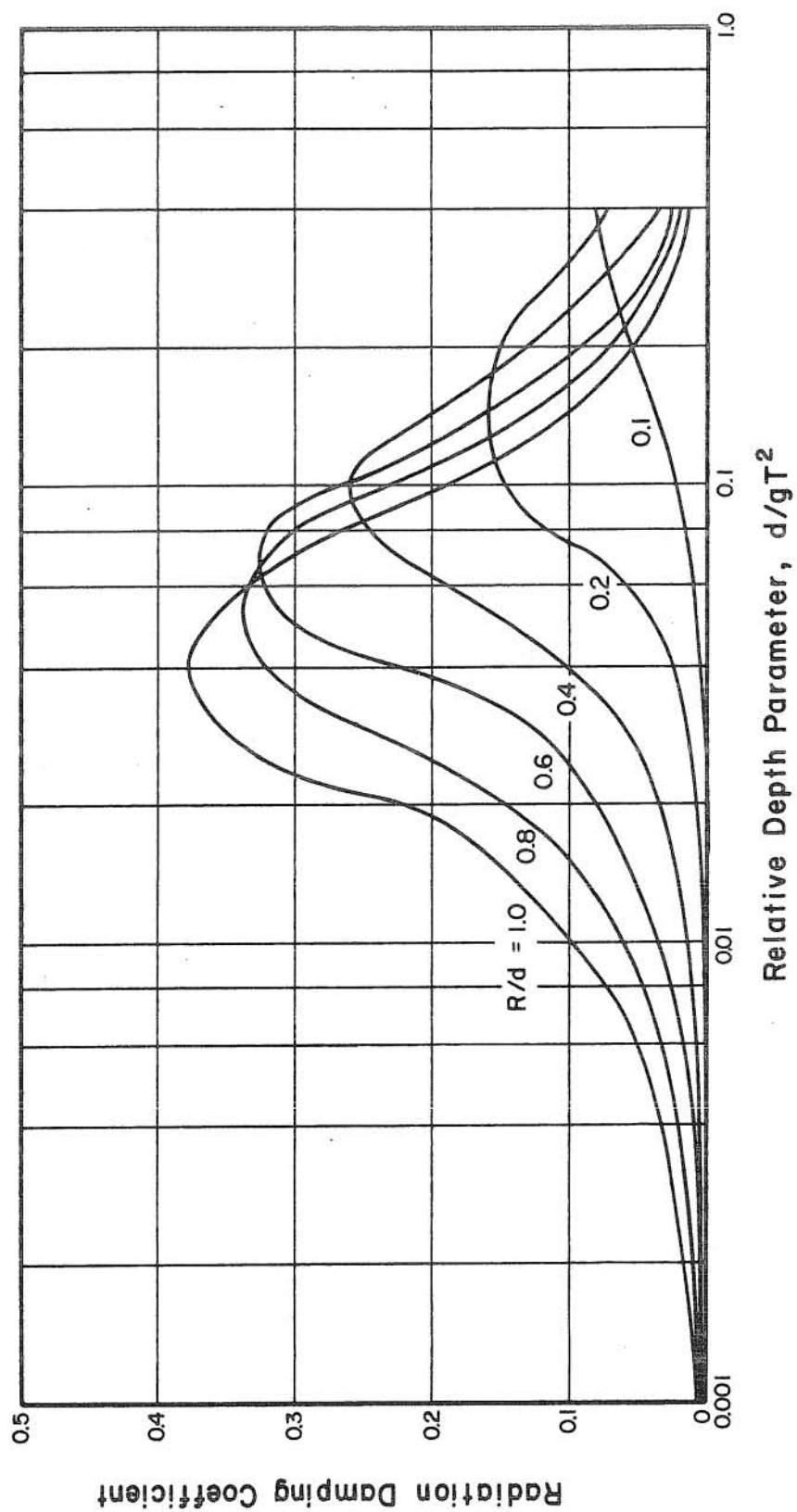


Fig. 4.1 Relationship Between the Radiation Damping Coefficient, C_R , and the Relative Depth Parameter, d/gT^2 , for Various Ratios of Cylinder Diameter to Water Depth, D/d , Triangular Mode Shape.

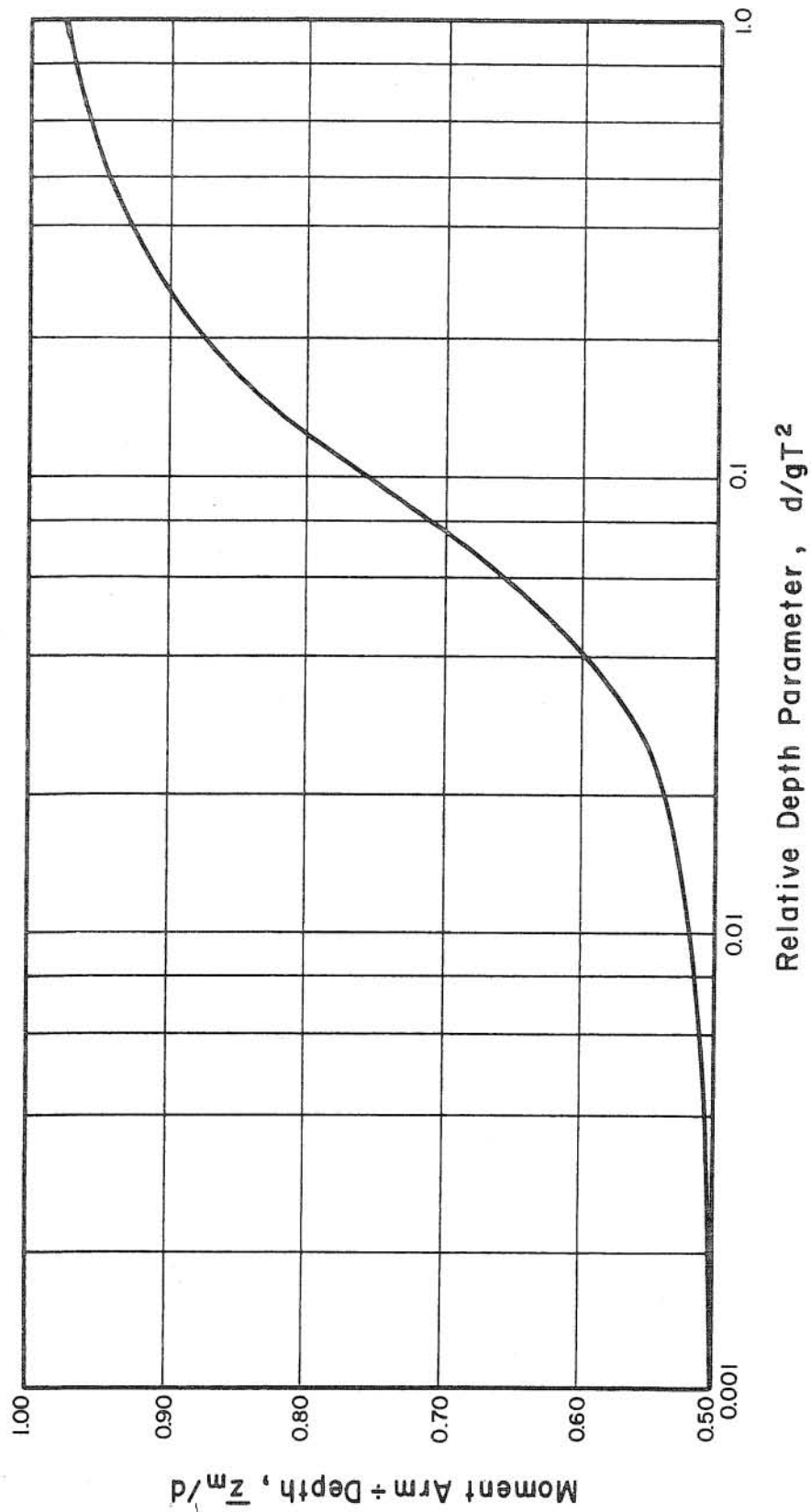


Fig. 4.2 Relationship Between the Ratio Radiation Damping Force of Moment Arm to Water Depth, \bar{z}_m/d , and the Relative Depth Parameter, d/gT^2 .

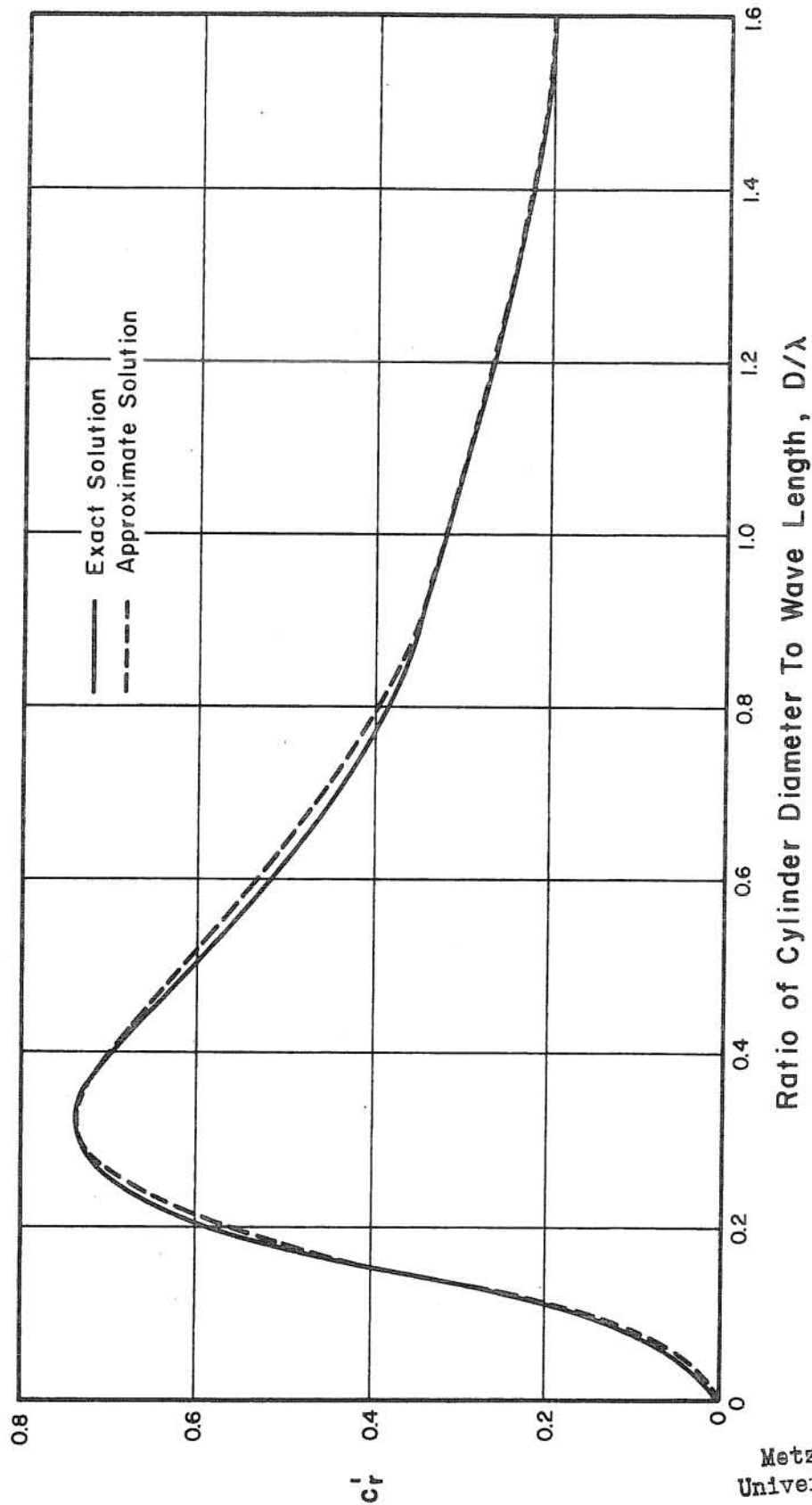


Fig. 4.3 Relationship Between the Coefficient c'_r and the Relative Depth Parameter, d/gT^2 . $c'_r = 2 / \{ \pi(kR)^2 \{ (J'_1[kR])^2 + (Y'_1[kR])^2 \} \}$

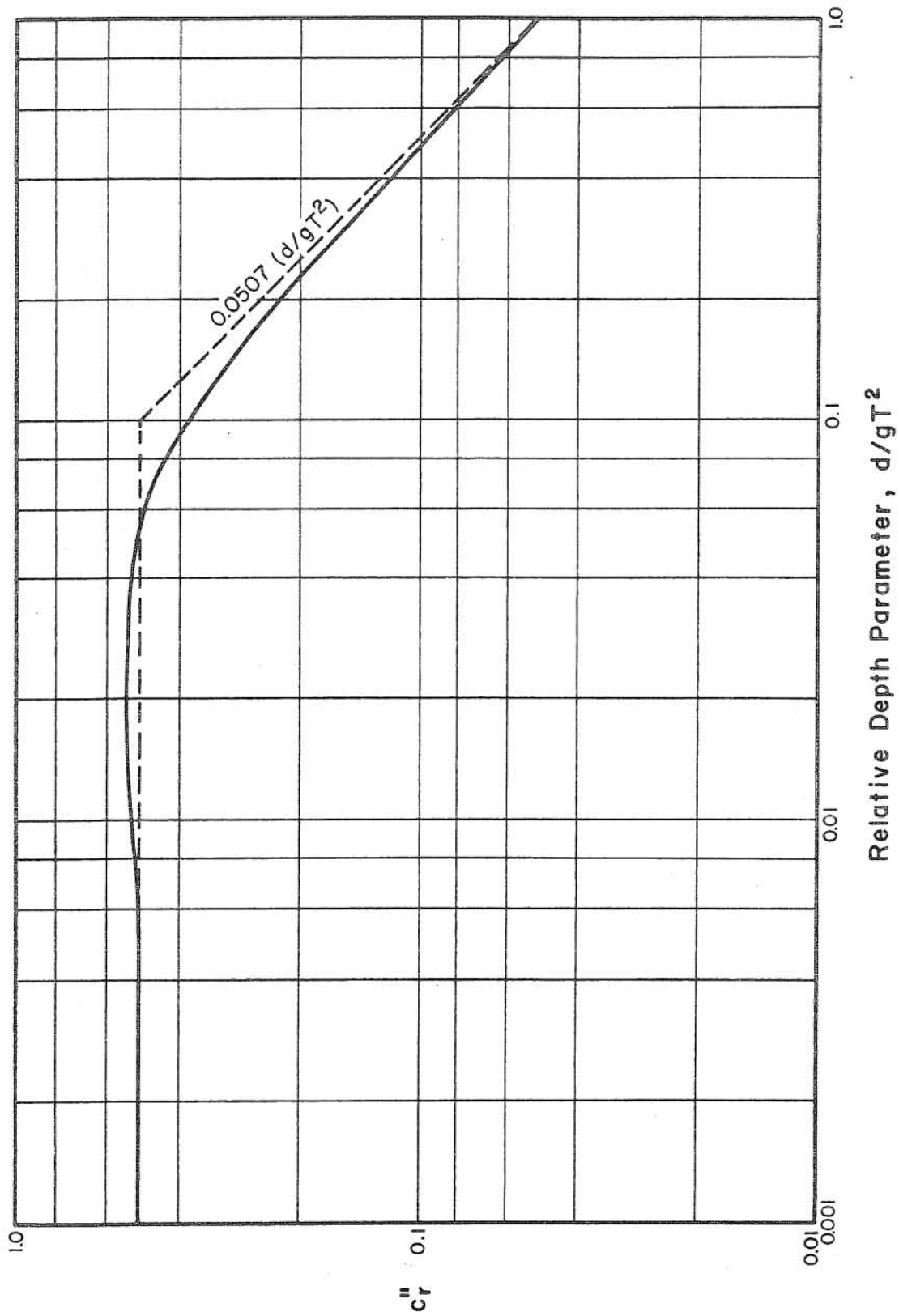


Fig. 4.4 Relationship Between the Coefficient c_r'' and the Relative Depth Parameter, d/gT^2 .
 $c_r'' = (I_3/I_4)(\sinh[kd]/kd)$.

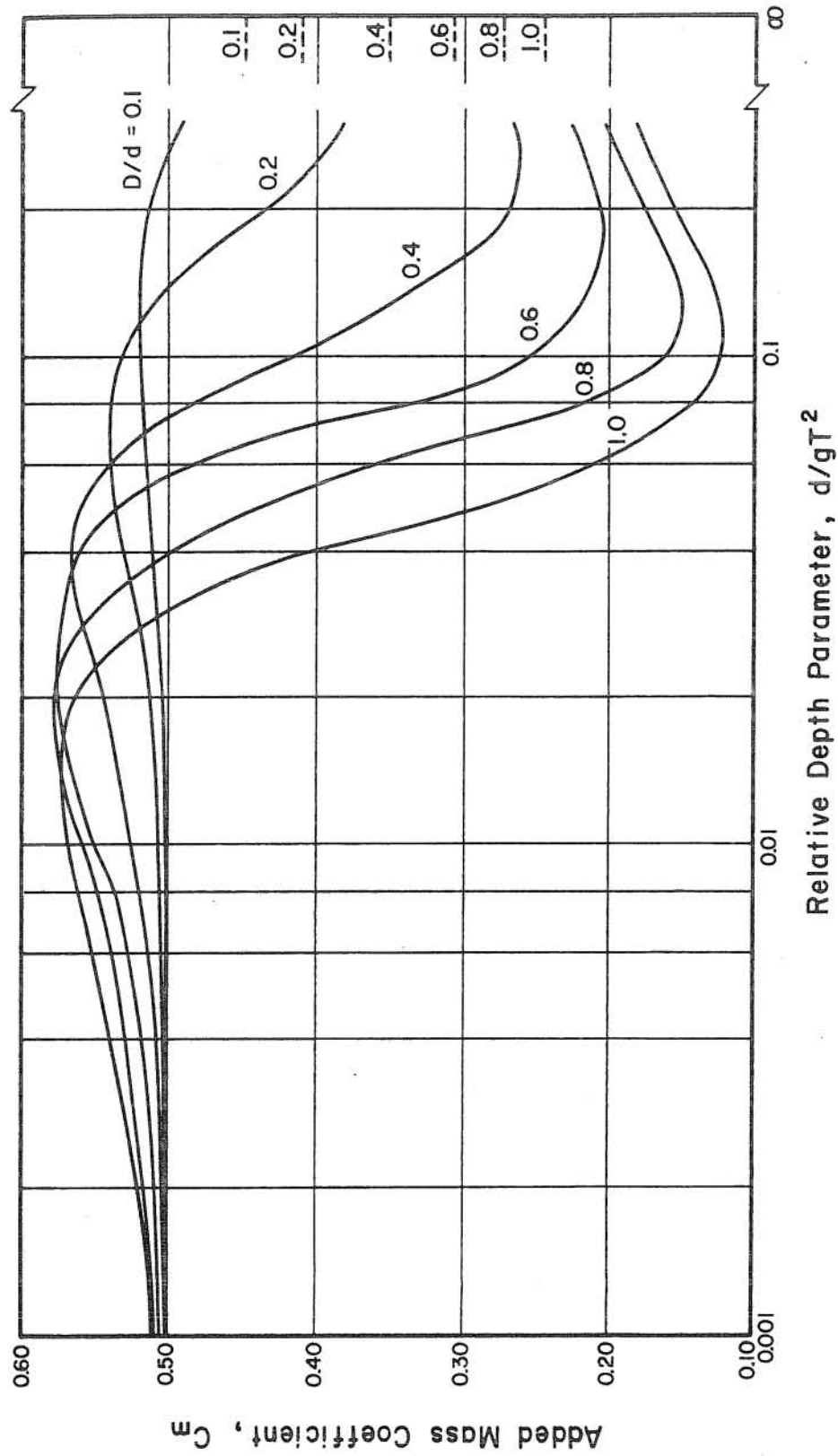


Fig. 4.5 Relationship Between the Added Mass Coefficient, C_M , and the Relative Depth Parameter, d/gT^2 , for Various Ratios of Cylinder Radius to Water Depth, D/d , Triangular Mode Shape.

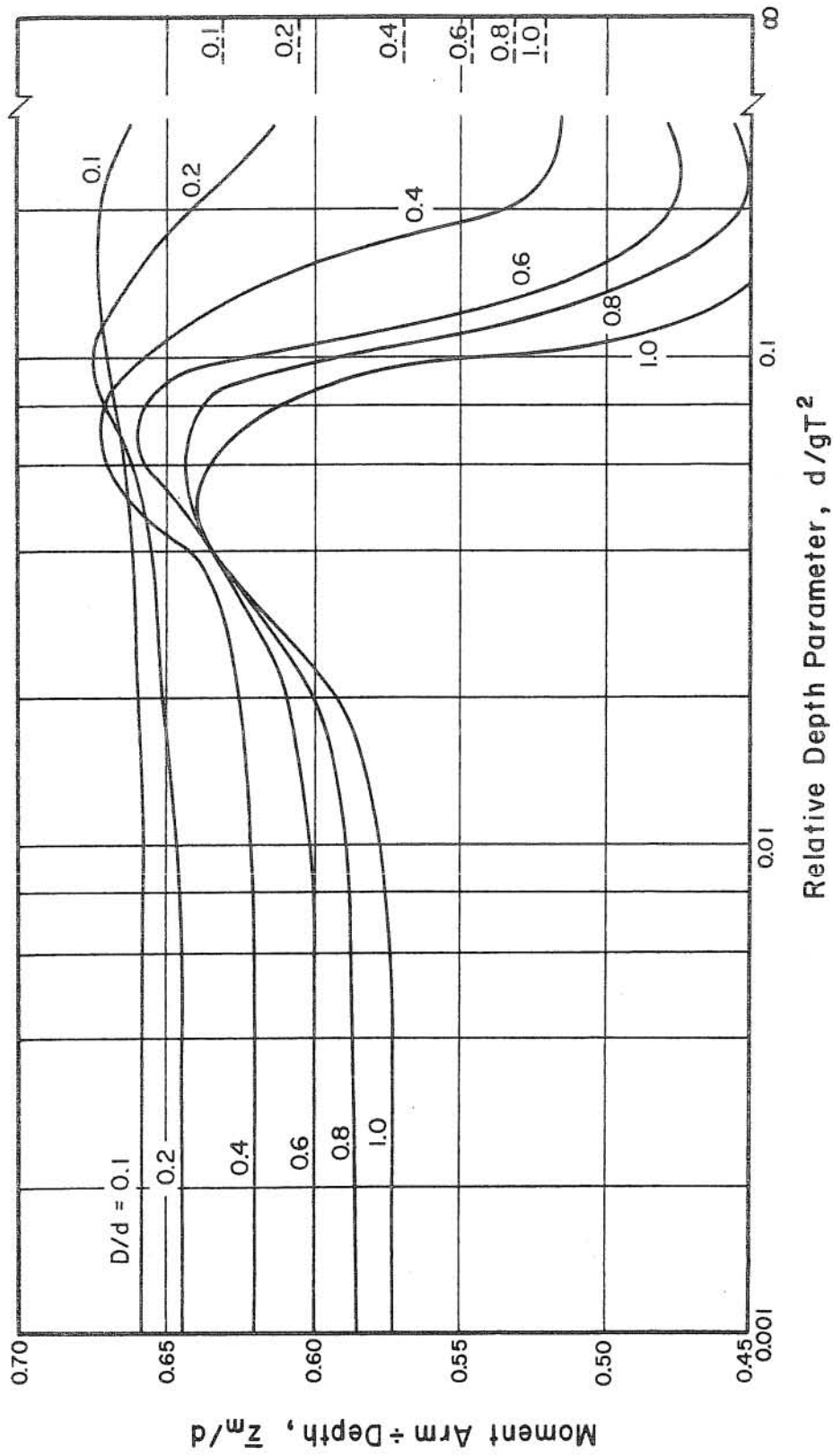


Fig. 4.6 Relationship Between the Ratio of Added Mass Force Moment Arm to Water Depth, z_m/d , and the Relative Depth Parameter, d/gT^2 , for Various Ratios of Cylinder Diameter to Water Depth, D/d , Triangular Mode Shape.

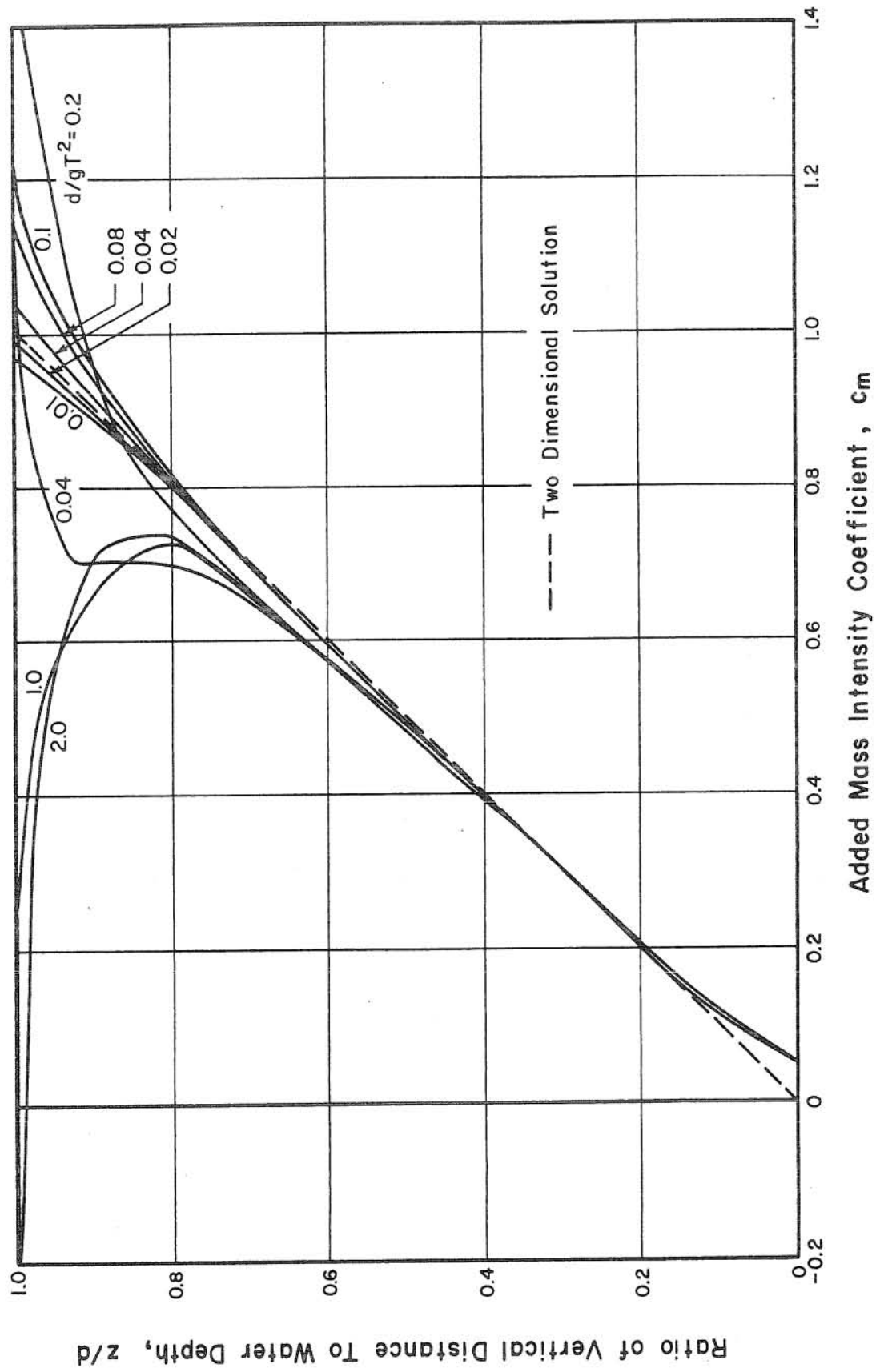


Fig. 4.7 Relationship Between Added Mass Intensity Coefficient, C_m , and Dimensionless Depth, z/d for a Cylinder Diameter to Water Depth Ratio, D/d , of 0.10 and Various Values of the Relative Depth Parameter, d/gT^2 , Triangular Mode Shape.

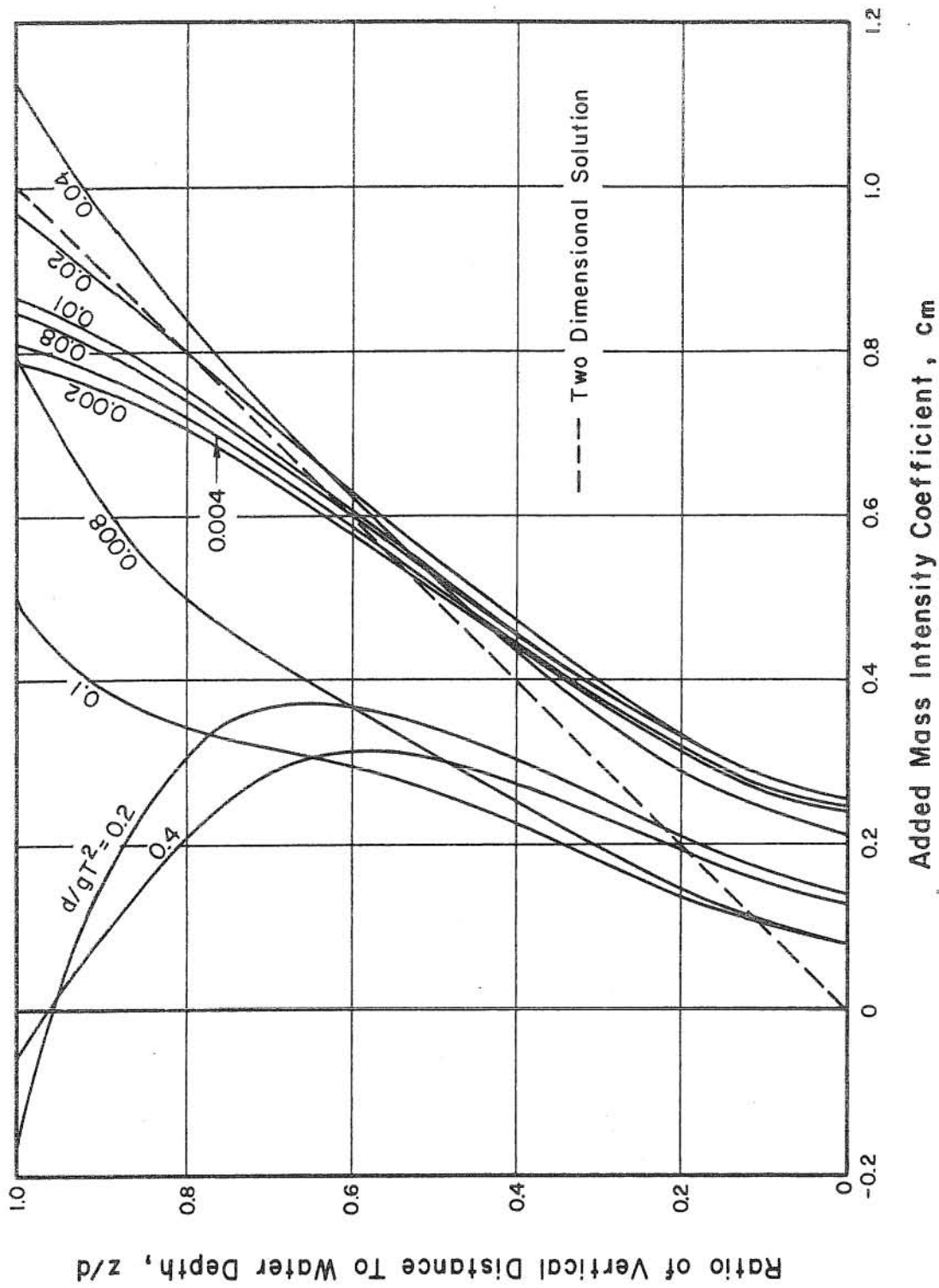
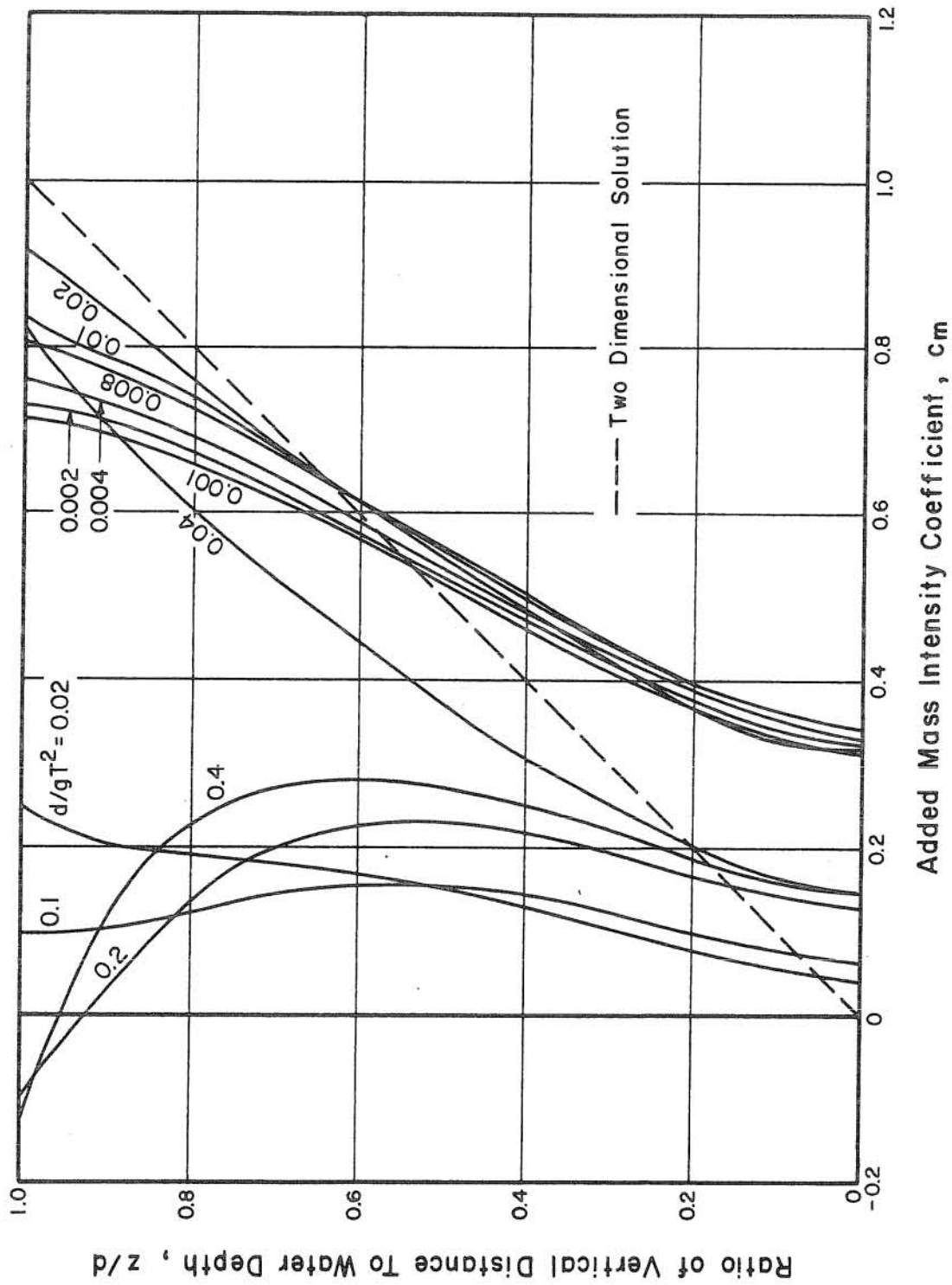


Fig. 4.8 Relationship Between Added Mass Intensity Coefficient, c_m , and Dimensionless Depth, z/d , for a Cylinder Diameter to Water Depth Ratio, D/d , of 0.6 and Various Values of the Relative Depth Parameter, d/gT^2 , Triangular Mode Shape.



4.9 Relationship Between the Added Mass Intensity Coefficient, C_m , and Dimensionless Depth, z/d , for a Cylinder Diameter to Water Depth Ratio, D/d , of 1.0 and Various Values of the Relative Depth Parameter, d/gT^2 , Triangular Mode Shape.

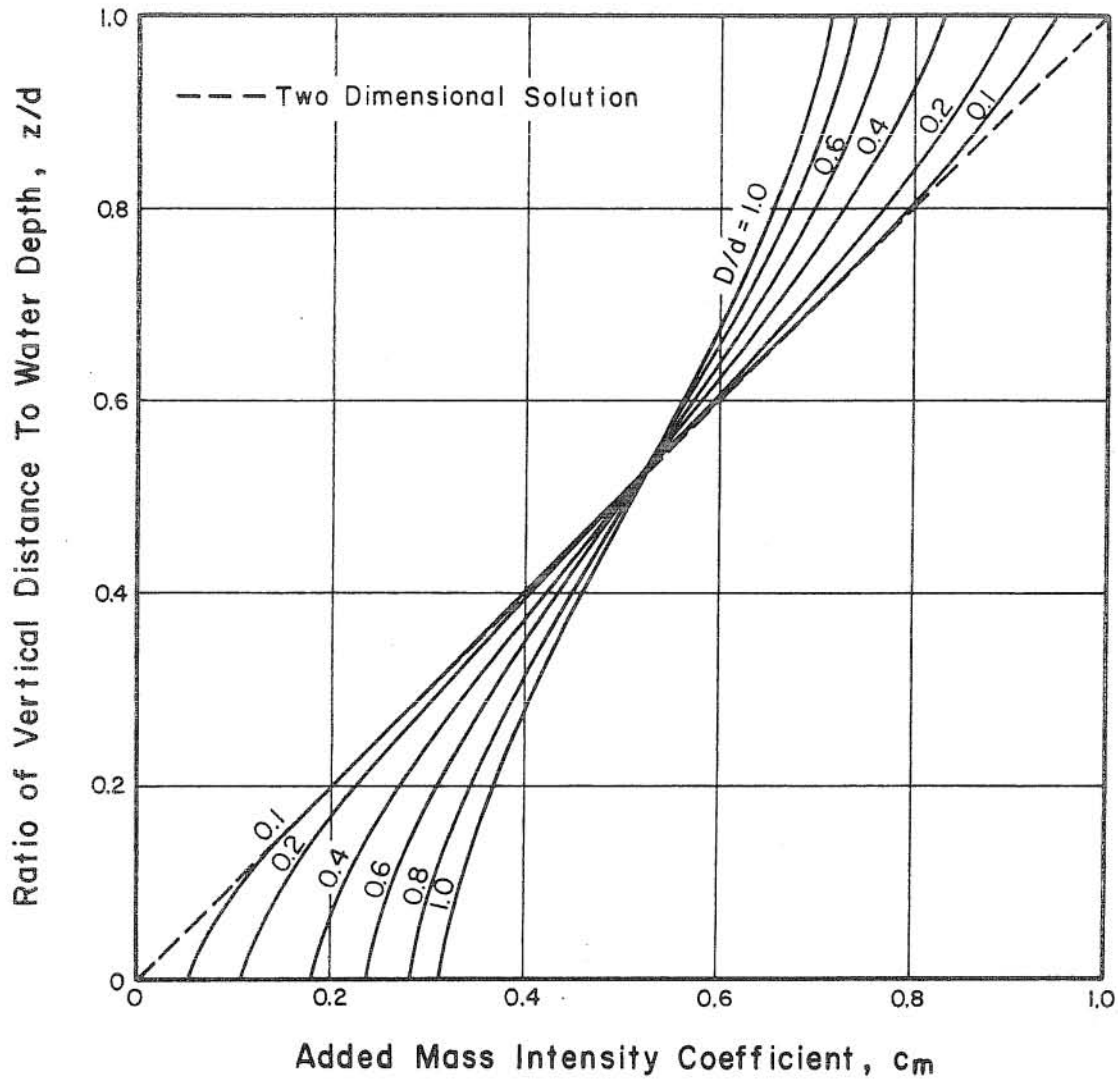


Fig. 4.10 Relationship Between the Added Mass Intensity Coefficient, c_m , and Dimensionless Depth, z/d , for a Relative Depth Parameter, d/gT^2 , of 0.001 and Various Values of the Ratio of Cylinder Diameter to Water Depth, D/d .

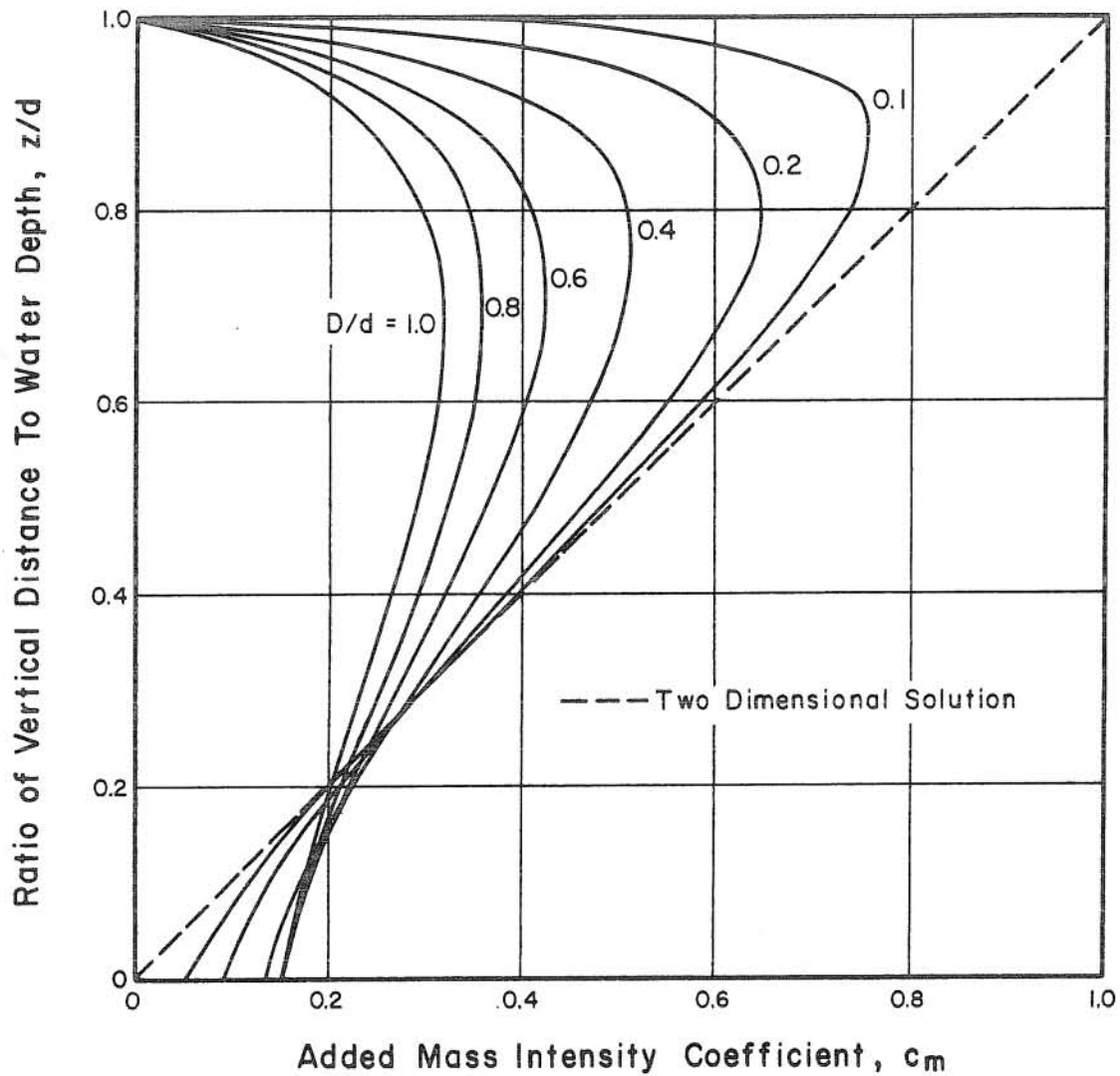


Fig. 4.11 Relationship Between the Added Mass Intensity Coefficient, c_m , and Dimensionless Depth, z/d , for a Relative Depth Parameter, d/gT^2 , of Infinity and Various Values of the Ratio of Cylinder Diameter to Water Depth, D/d .

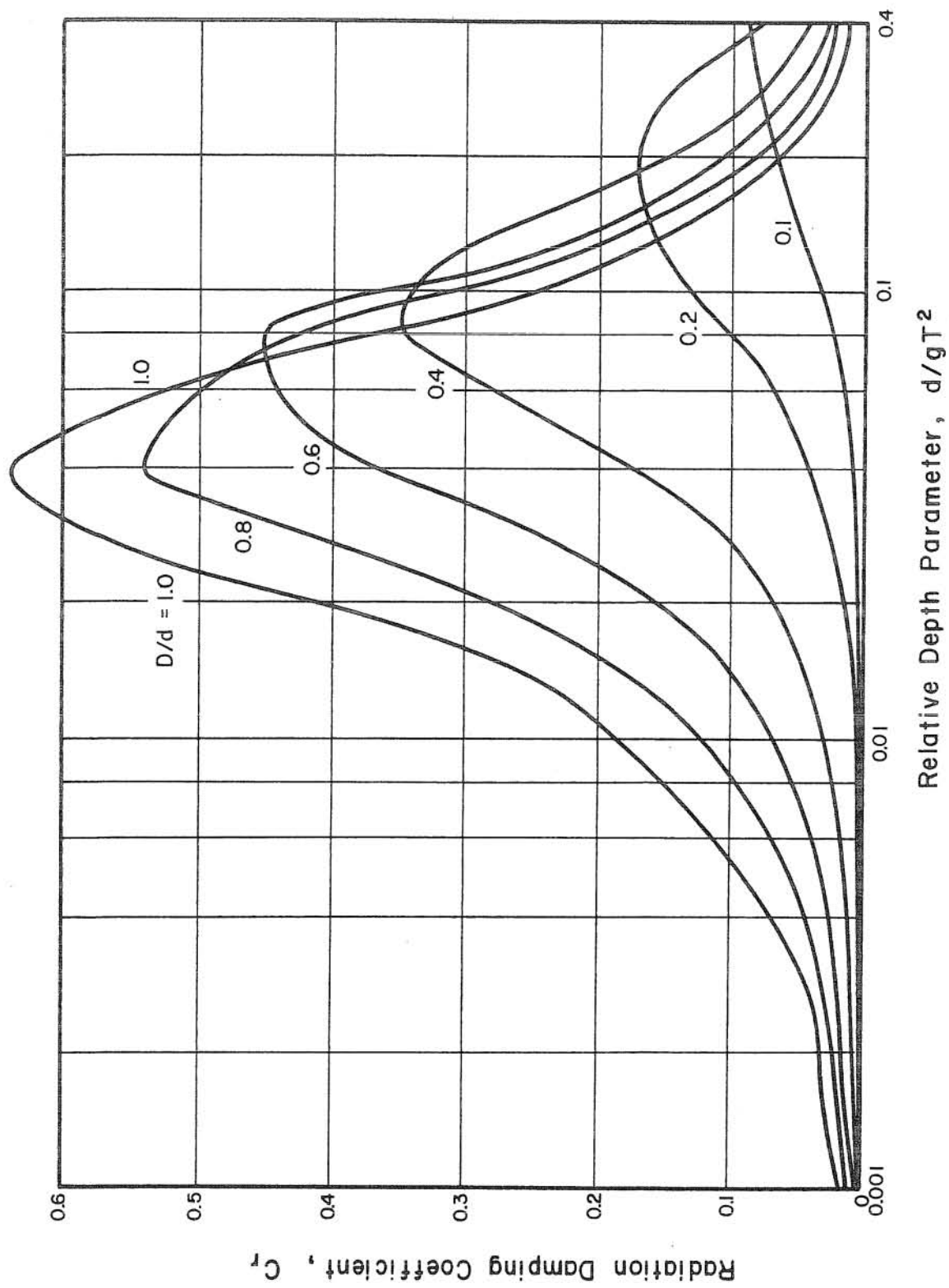


Fig. 4.12 Relationship Between the Radiation Damping Coefficient, C_r , and the Relative Depth Parameter, d/gT^2 , for Various Ratios of Cylinder Diameter to Water Depth, D/d , Translational Mode Shape.

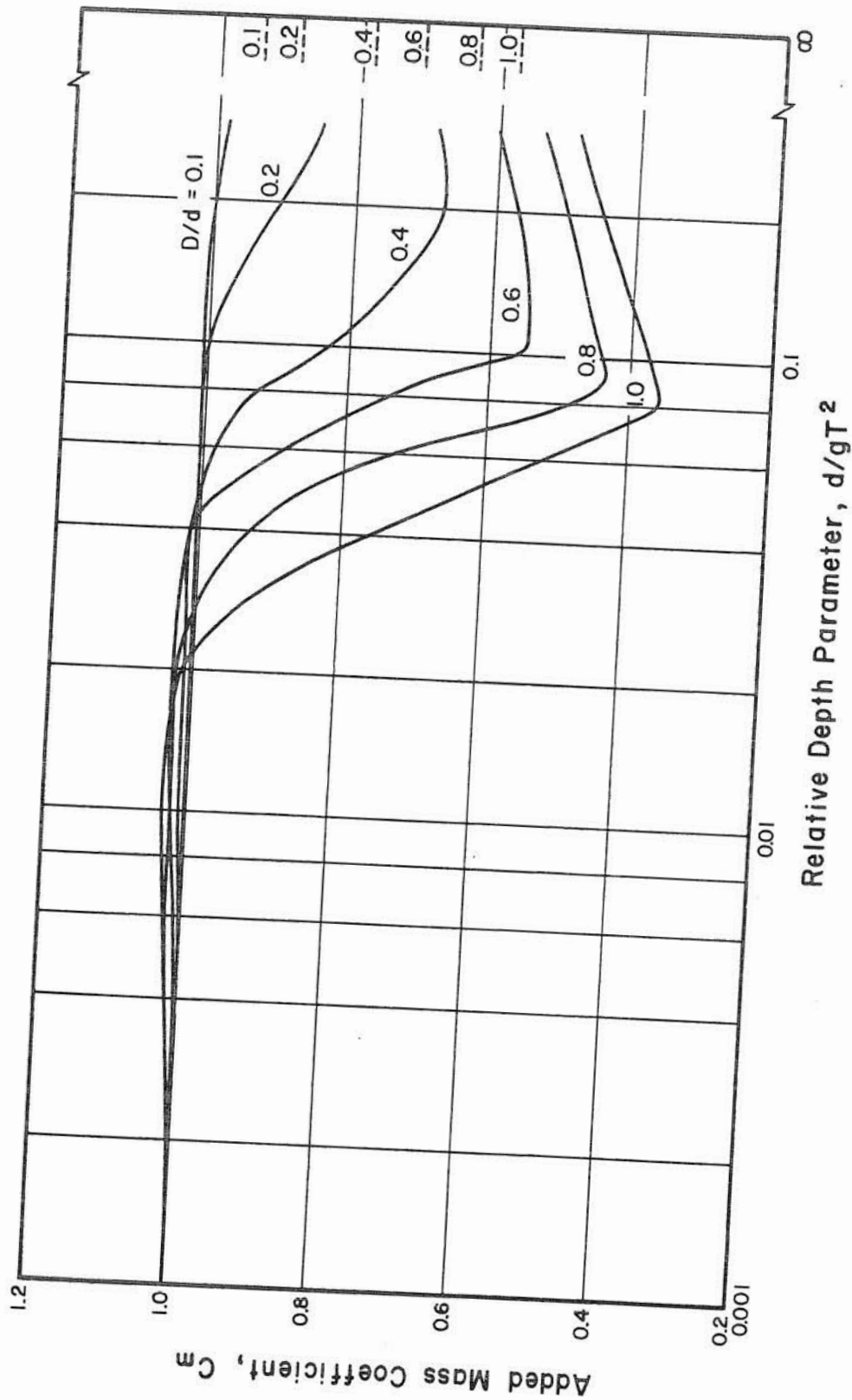


Fig. 4.13 Relationship Between the Added Mass Coefficient, C_m , and the Relative Depth Parameter, d/gT^2 , for Various Ratios of Cylinder Radius to Water Depth, D/d , Translational Mode Shape.

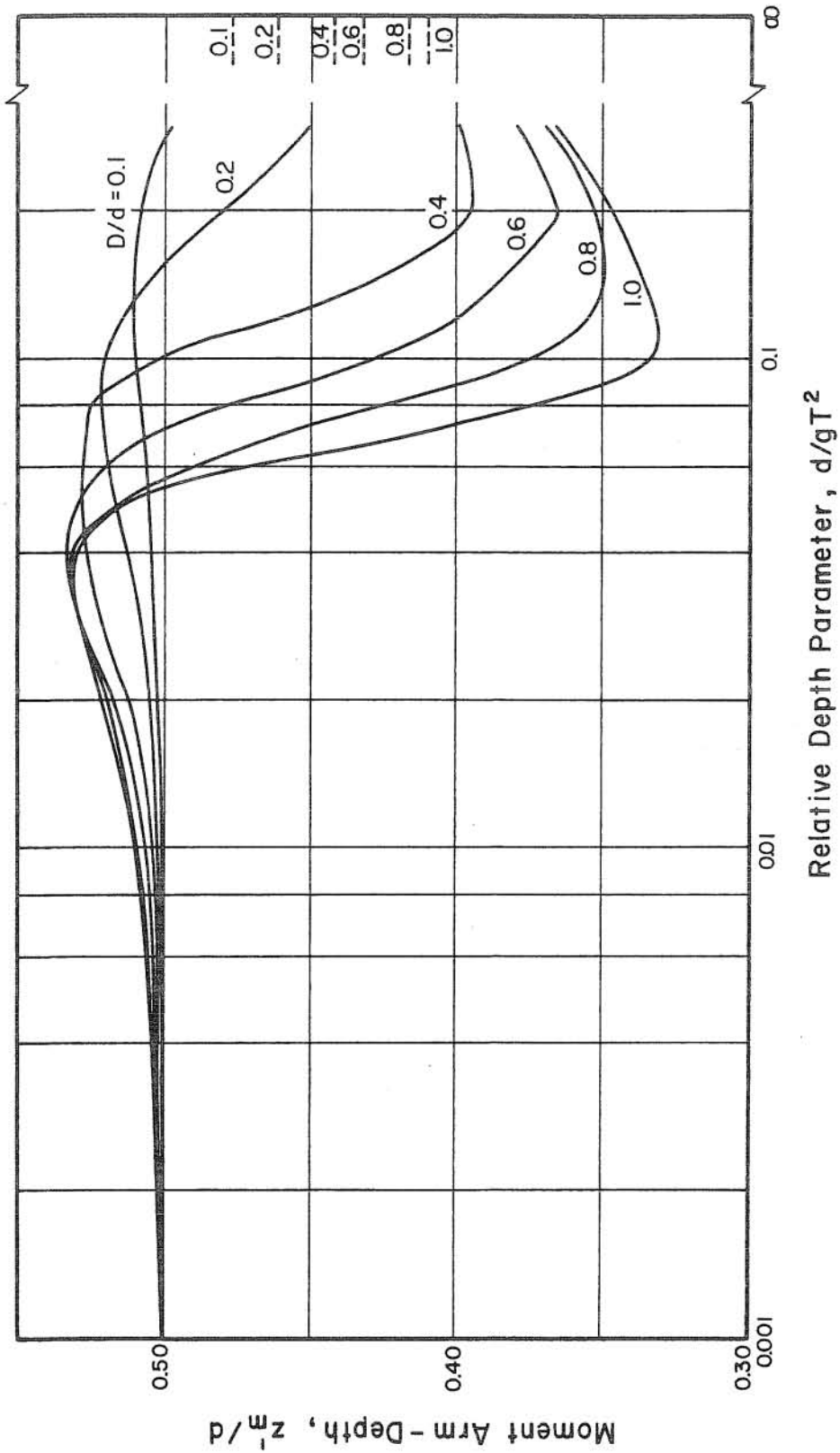


Fig. 4.14 Relationship Between the Ratio of Added Mass Force Moment Arm to Water Depth, z'_m/d , and the Relative Depth Parameter, d/gT^2 , for Various Ratios of Cylinder Diameter to Water Depth, D/d , Translational Mode Shape.

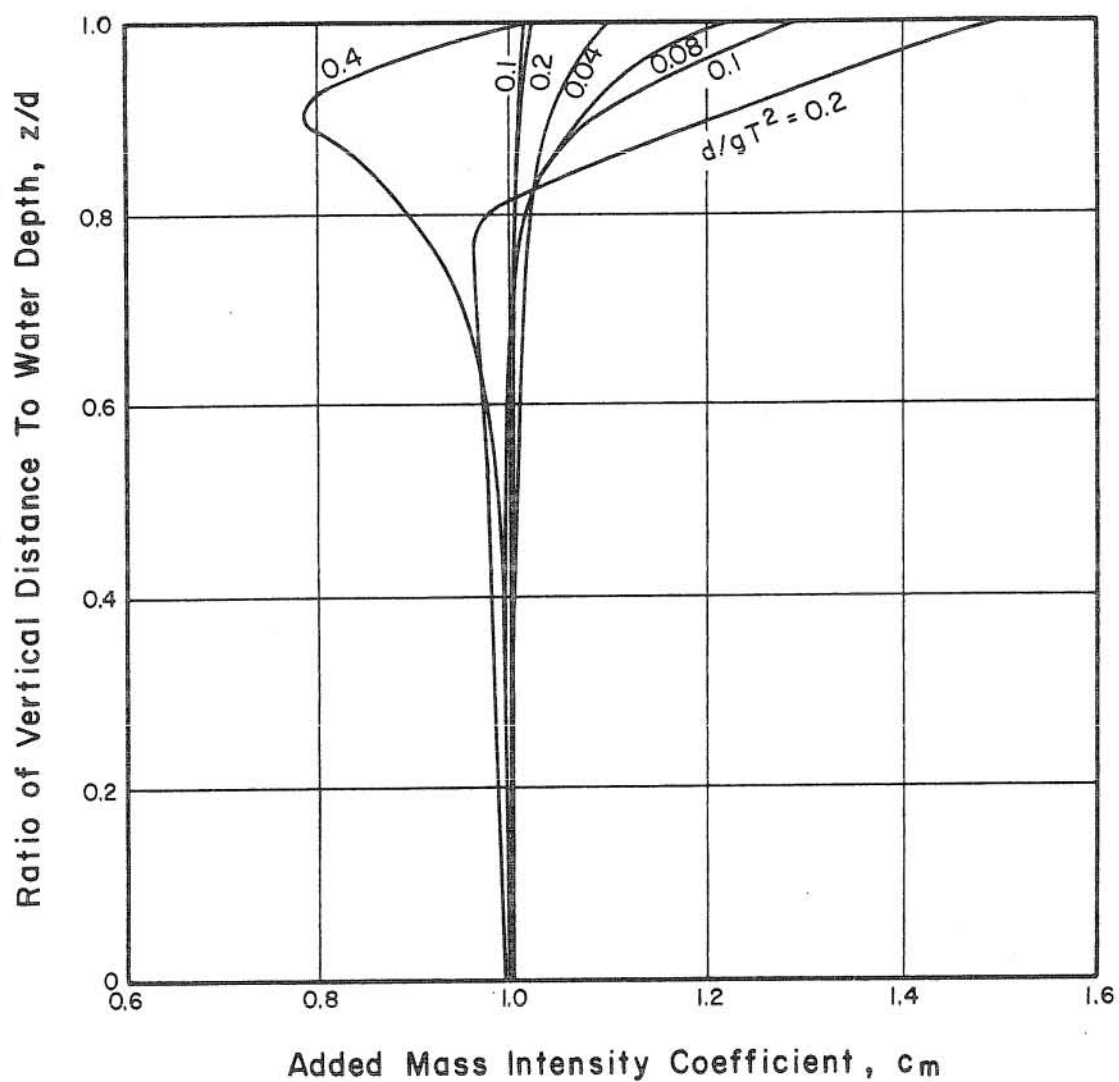


Fig. 4.15 Relationship Between Added Mass Intensity Coefficient, c_m , and Dimensionless Depth, z/d , for a Cylinder Diameter to Water Depth Ratio, D/d , of 0.10 and Various Values of the Relative Depth Parameter, d/gT^2 , Translational Mode Shape.

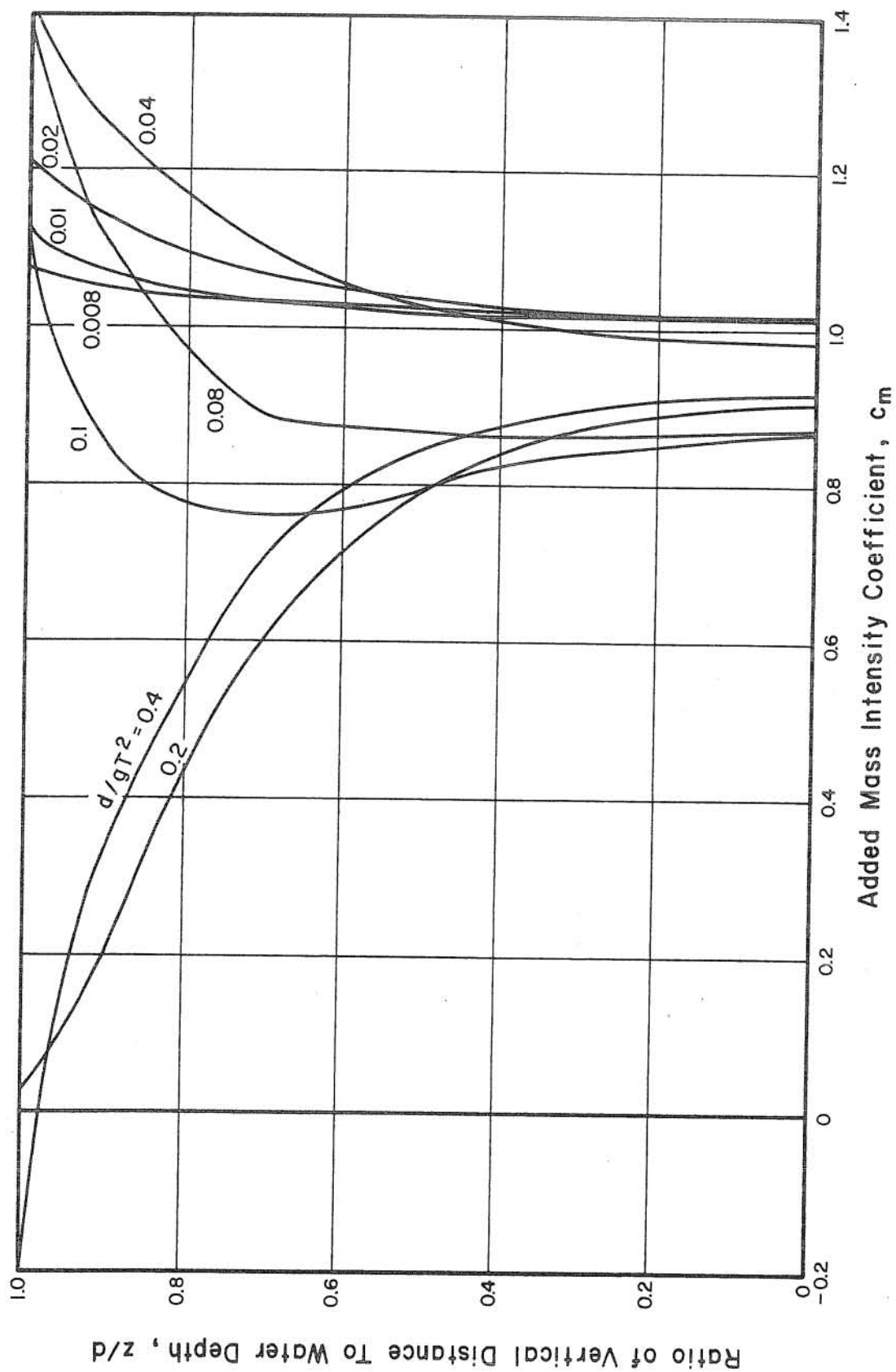


Fig. 4.16 Relationship Between Added Mass Intensity Coefficient, C_m , and Dimensionless Depth, z/d , for a Cylinder Diameter to Water Depth Ratio, D/d , of 0.4 and Various Values of the Relative Depth Parameter, d/gT^2 , Translational Mode Shape.

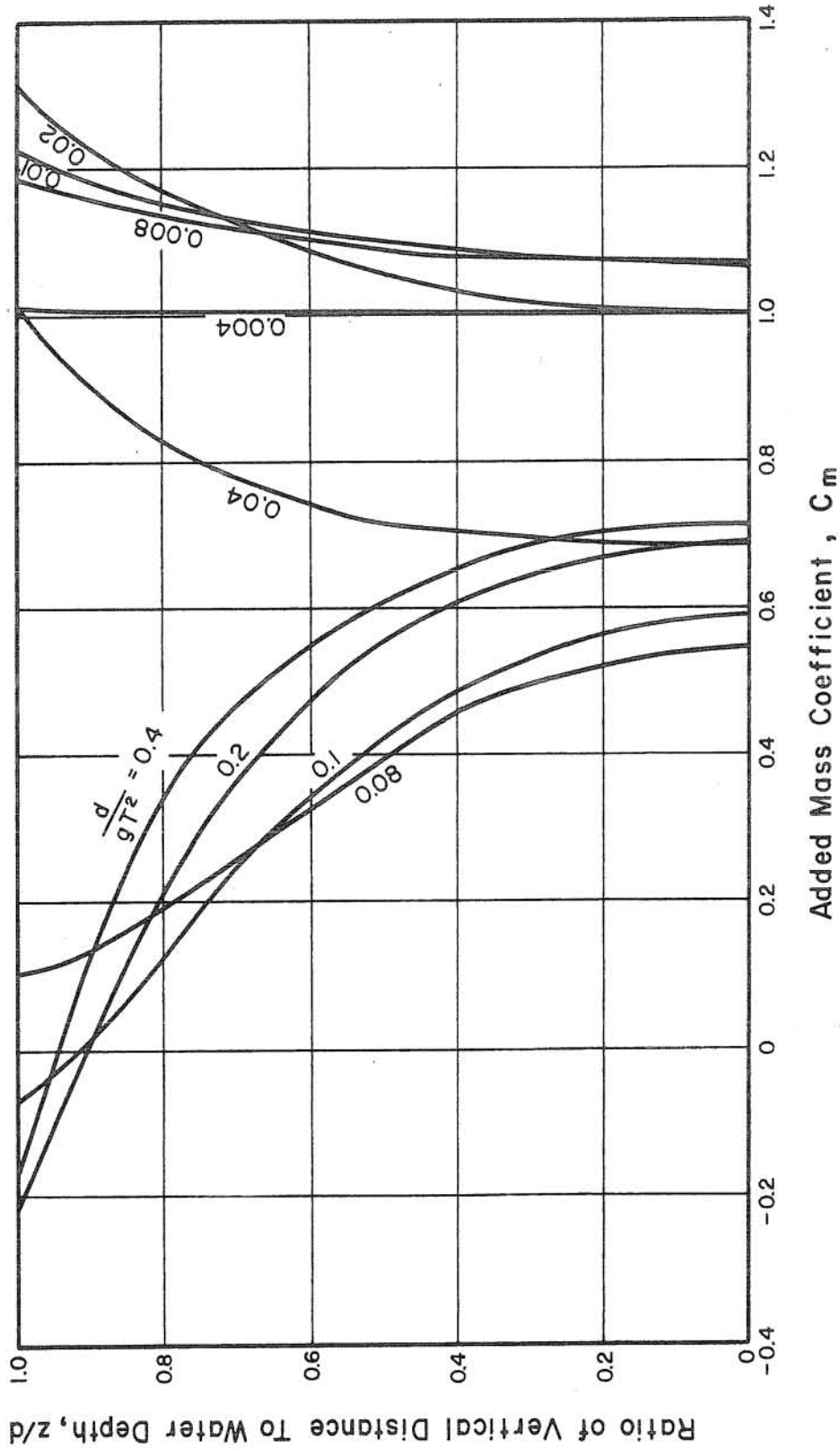


Fig. 4.17 Relationship Between the Added Mass Intensity Coefficient, C_m , and Dimensionless Depth, z/d , for a Cylinder Diameter to Water Depth Ratio, D/d , of 1.0 and Various Values of the Relative Depth Parameter, d/gT^2 , Translational Mode Shape.

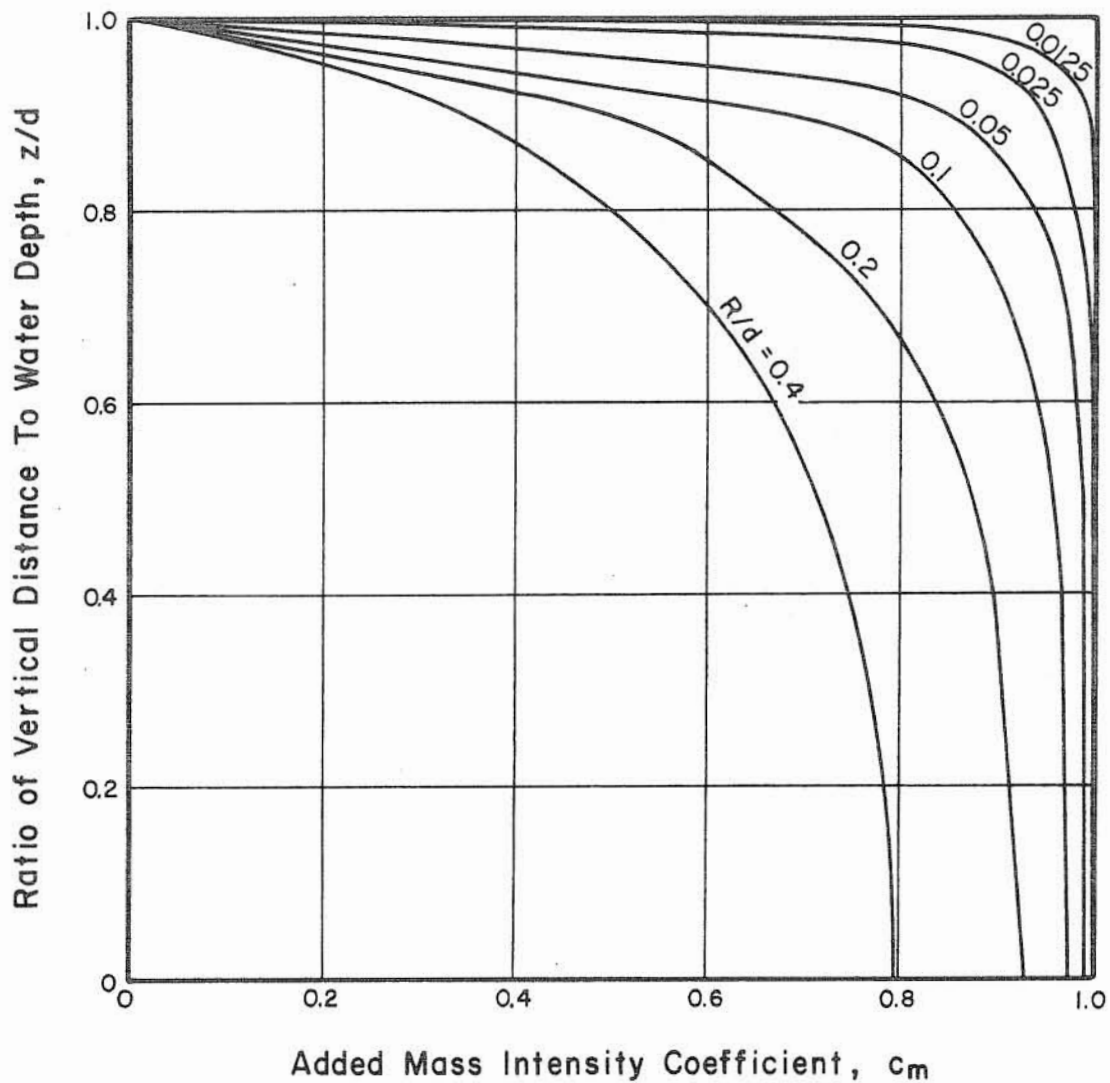
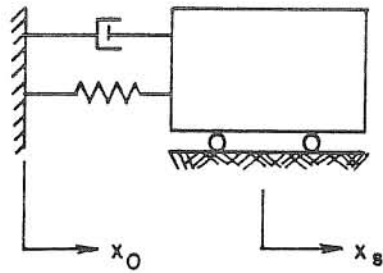
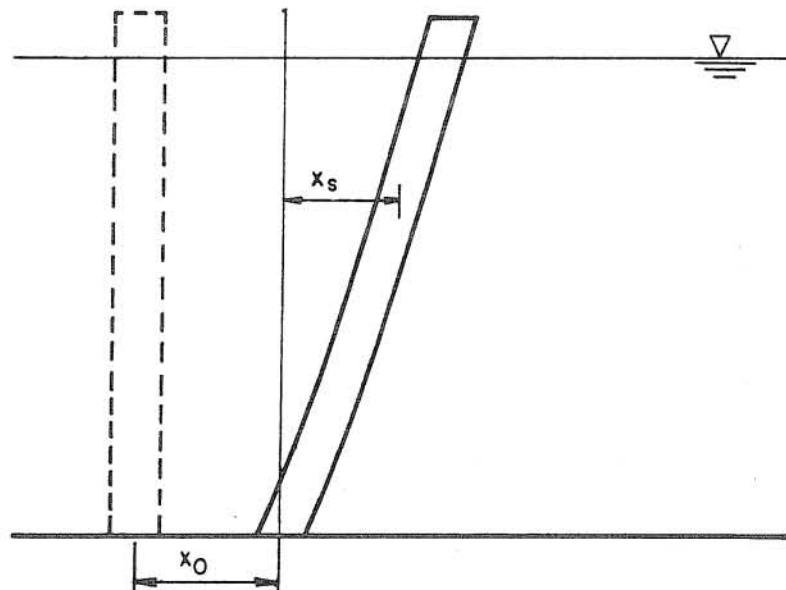


Fig. 4.18 Relationship Between the Added Mass Intensity Coefficient, c_m , and Dimensionless Depth, z/d , for a Relative Depth Parameter, d/gT^2 , of Infinity and Various Values of the Ratio of Cylinder Diameter to Water Depth, D/d , Translational Mode Shape.



(a) Single Degree - of - Freedom System



(b) Multi Degree - of - Freedom System

Fig. 5.1 Definition Sketch for Structures Subjected to Horizontal Ground Motion.

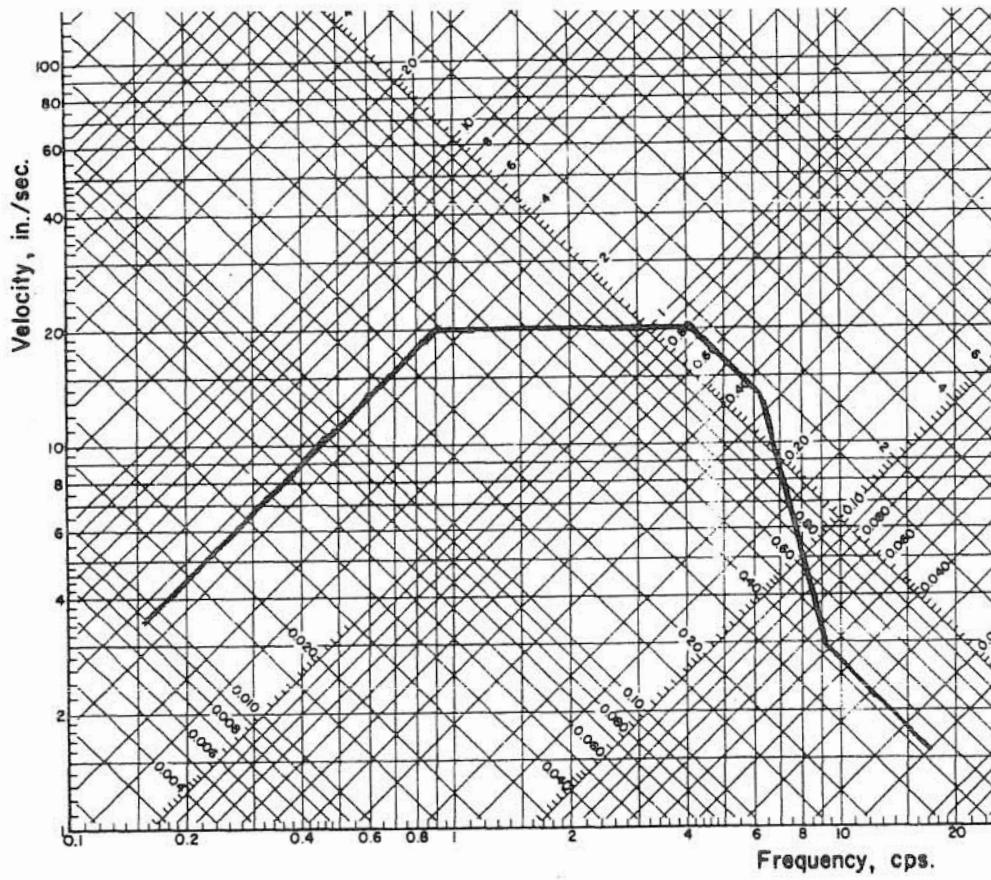


Fig. 5.2 Idealized Structural Response Spectrum

BIBLIOGRAPHY

1. Lamb, H., Hydrodynamics, Dover Edition, 1945.
2. Havelock, T. H., "The Pressure of Water Waves Upon a Fired Obstacle," Proc. Roy. Soc., Vol. 175 A., July 1940.
3. McCamy, R. C. and Fuchs, R. A., Wave Forces on Piles: A Diffraction Theory, TM No. 69, Beach Erosion Board, Office of the Chief of Engineers, 1954.
4. Spring, B. W. and Monkmeyer, P. L., "Interaction of Plane Waves with a Row of Cylinders," Proc. Civil Engineering in the Oceans III, A.S.C.E., 1975, p. 979-998.
5. Biéssel, F., et al., "Laboratory Wave-Generating Apparatus," English Translation from La Houille Blanch by St. Anthony Falls Hydraulic Laboratory, U. of Minn. Proj. Rep. No. 39, March 1954.
6. Petruskas, C., Hydrodynamic Damping and "Added Mass" for Flexible Offshore Platforms, Ph.D. Thesis, University of California, Berkeley, 1973.
7. Liaw, C. Y. and Chopra, A. K., "Dynamics of Towers Surrounded by Water," Earthquake Engineering and Structural Dynamics, Vol. 3, 1974, p. 33-49.
8. Jacobson, L. S., "Impulsive Hydrodynamics of Fluid Inside a Cylindrical Tank and of Fluid Surrounding a Cylindrical Pier," Bull. Seism. Soc. Am. 39, 1949, p. 189-204.
9. Ippen, A., Estuary and Coastline Hydrodynamics, McGraw-Hill, 1966.
10. Newmark, N. M. and Rosenblueth, E., Fundamentals of Earthquake Engineering, Prentice-Hall, 1971.

